On the preservation of climate variations in the stratigraphic record

Timo Millenaar

May 26, 2020

Abstract

In stratigraphic studies, basin deposits are often used as a proxy for climatic variations. Understanding which climatic variations are likely to be recorded in these deposits is vital to their interpretation. Previous studies showed that proximal sediment input variations are unlikely to be recognisably preserved in the stratigraphic record at the end of the alluvial system. However, the role of a simultaneously varying sediment transport capability of the sedimentary system is unknown. An open source numerical model is developed and used in this study to investigate how various climatic variations are treated by, and recorded in, an alluvial fan. A focus lies on varying the general sediment redistribution capability of the system in sync with the sediment input into the system.

The results presented in this paper indicate that input signals form the catchment area are indeed buffered by an alluvial fan. Sediment leaving the fan at its distal end does however directly reflect both rapid (tens to hundreds of thousands of years) and long (millions of years) changes in climatic forcing. This is facilitated by changes in the sediment transport capability of the system. The distal end of the system therefore immediately experiences increases and decreases in the amount of sediment leaving the system. A single climate signal can therefore create a two step change in the output signal of the alluvial fan. The first step is then related to a direct increase of the sediment transport rate and the second step is related to the delayed arrival of sediment derived from the catchment area.

It was also found that, within the alluvial fan, gravel front propagations generally occur in two scenarios. The first scenario involves a prolonged scarcity of new sediment input, which allows coarse material to travel downstream for it is not being covered by or diluted with newly arriving sediment. The second scenario involves a rapidly increasing sediment transport capability over input ratio, which can transport coarse material downstream before it is covered by newly arriving sediment.

1 Introduction

1.1 Relating external forcing to stratigraphy

The conditions in the sedimentary system at the time of deposition determine the structure and composition of the sedimentary deposits that make up the stratigraphic record. Past changes in external forces and processes acting on the sedimentary system, or forcing mechanisms, could therefore be recognised in the stratigraphic record, if preserved. These forcing mechanisms are often broadly separated into climatic forcing and tectonic forcing. A common goal of many stratigraphic studies is thus, unsurprisingly, to infer past changes and conditions of external forcing mechanisms from the stratigraphic record. This information is crucial, for example, to formulate understanding about the long term effects of changes in climate. Interpreting past conditions from the stratigraphic record is, however, not trivial. It requires thorough understanding of the interactions between the governing forces, the sedimentary system in question and the resulting stratigraphy.

1.2 A conceptual model

In order to improve this understanding, many recent publications discussed the extent to which variations in forcing of different timescales are recorded in the stratigraphic record (Castelltort and Van Den Driessche, 2003; Allen, 2008; Jerolmack and Paola, 2010; Romans et al., 2016; Watkins

et al., 2018). The implication being that forcing variations operating at certain timescales can not be properly reconstructed using the stratigraphic record as a proxy, if variations at those timescales are often not recognisably recorded in the stratigraphic record.

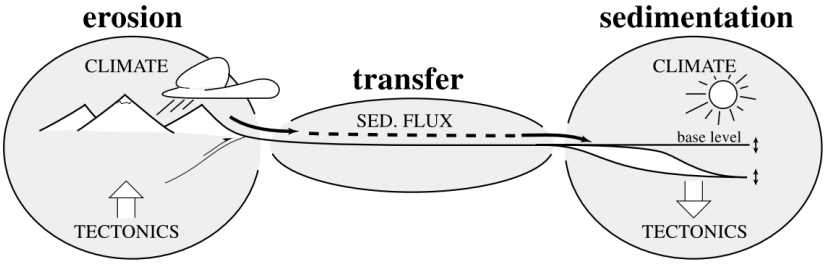

Figure 1: The simplified conceptual model of a sediment transfer system from (Castelltort and Van Den Driessche, 2003). The sediment fluxes entering and leaving the transfer system are considered *input* and *output*, respectively.

These studies are predicated on the conceptional model that a given sedimentary system has sediment input at the proximal side, sediment output at the distal side and can deposit sediment in, or erode sediment from, its corresponding stratigraphy. Using this conceptual model, relations between external forcing mechanisms and the stratigraphy are sought.

This concept can be simplified further by disregarding any erosion or deposition within the transfer system as is done by Castelltort and Van Den Driessche (2003), see figure 1.

In such models, boundary conditions that are dependent on time, such as the sediment input, are often referred to as signals. As sediment is transported through the sedimentary system in question, the signal is carried with it and could be recognised in the output signal. These signals can be an aggregate of individual sub-signals, with a specific period and amplitude. Each of these sub-signals can have its own origin, such as a specific orbital cycle. For a more elaborate description of signals in sedimentary systems, the reader is referred to (Romans et al., 2016).

In the hypothetical case that the downward slope in the sedimentary system is constant, and thus no erosion or deposition occurs, nor any accommodation space is created, the output should strongly reflect the input. Mass, after all, is to be conserved. There are however many ways in which the signal can be convoluted during transportation, such as the storage and release of sediment along the way. For the purposes of this research I mostly focus on the influence of time and whether the frequency of a signal influences its chances of being recognisably preserved in the stratigraphic record.

1.3 A sense of time

When the height profile from one end of a sedimentary system to another is stable, and thus does not vary with time, it can be said to be in equilibrium. It can very reasonably be argued that no natural system is subject to stagnant boundary conditions and thus can never truly be in equilibrium. For all practical purposes, i will speak of a near-equilibrium state when the changes occur slow enough for the system to be able to keep up. The height profile would then still reflect the current boundary conditions at any moment in time. The time it takes for a system to reach its near-equilibrium state is specific for each variety of sedimentary system (Allen, 2008), and is generally referred to as the 'equilibrium time' or 'response time' of the system.

An important factor controlling the equilibrium time is the ability to redistribute sediment. This is ability of a system to redistribute sediment is often referred to as the diffusivity. It includes all major and minor processes, excluding hill slope, that influence sediment transport rate such as precipitation rate, vegetation cover, bioturbation and viscosity.

For an alluvial fan, this equilibrium time (T_{eq}) is generally in the order of hundreds of thousands of years up to about a million years Paola et al. (1992); Allen (2008) and can be approximated by:

$$T_{eq} \sim L^2 K^{-1} \tag{1}$$

Here, L is the length of the system in m and K is the diffusivity constant in $m^2 s^{-1}$. If the period of the forcing signal is shorter in duration then T_{eq}, the change is considered to be rapid or high-frequency. Changes with longer periods are considered to be slow or low-frequency.

Sediment redistribution mechanisms inherent to the system, like landslides, are likely to destroy signals with a period that is shorter than the average time between events (Jerolmack and Paola, 2010), unless the magnitude is sufficiently high. Tectonic and climatic variations however, mostly occur at timescales larger then most system-specific timescales. System specific timescales for terrestrial sediment routing systems, usually in the order of seconds (eddy turnover time) to some hundreds of years (landslides), are not considered further in this paper. 'High-frequency' in this paper therefore refers to timescales of thousands of years up to about a million years, the upper limit being dependent on equation 1. Signals with a period that is longer then the equilibrium time are termed 'low-frequency'.

1.4 Signal preservation and manipulation

It was suggested by both Castelltort and Van Den Driessche (2003) and Allen (2008) that high-frequency changes in the amount of sediment leaving the catchment area are dampened by a transfer system between the source area and the depositional basin, such as shown in figure 1. The dampening effect that the transfer system has on the input signal decreases the likelihood that the stratigraphy in the sink at the distal end of the transfer system reflects these high-frequency sediment input signals.

Such a transfer system can also create a delay, or phase-shift, between sediment in- and output signals (Jerolmack and Paola, 2010; Watkins et al., 2018). This complicates the interpretation of the relation between a given distal sedimentary deposit and erosion in the catchment area. Accommodation space creation due to subsidence may, however, allow information about forcing signals to be stored in the transfer system as well. Climatic changes can, for example, be recognised in changes in the gravel front location within an alluvial fan, (Paola et al., 1992). Alluvial fans therefore not only functions as a potential buffer, similar the transfer system shown in figure 1, but may also record signals that may be less recognisable in more distal deposits. Since alluvial fans capture all these concepts, I will limit the scope of this study to alluvial fans only, for practical purposes. The concepts, applied to an alluvial fan setting, are visualised in figure 2.

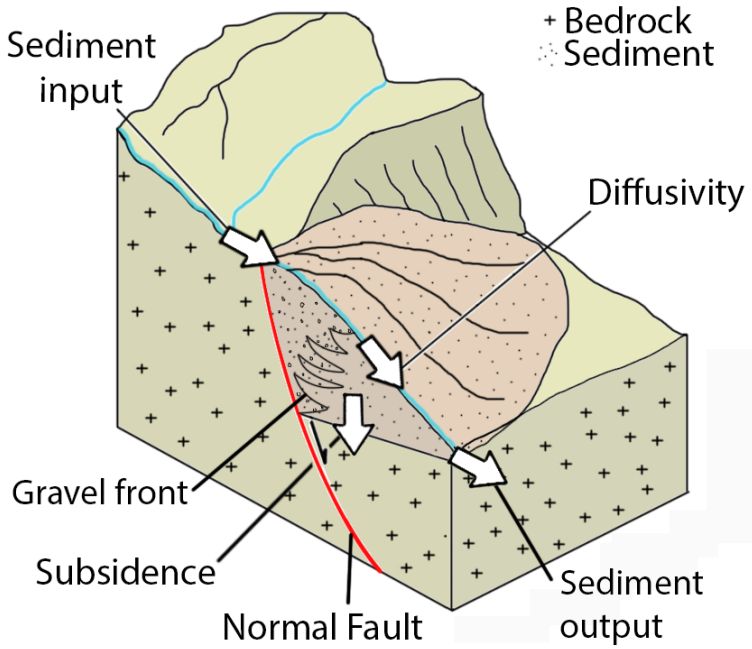

Figure 2: A scenario showcasing the general geological setting and corresponding boundary conditions included in the model

1.5 Importance of sediment diffusivity versus input

It is important to consider that changes in climate not only effect the sediment input into the transfer system, but also affect the discharge and therefore the transport rate of the transfer system. This is demonstrated by the findings of Watkins et al. (2018), who investigated if high-frequency changes in the climate can be recognised in deposits in a confined system in the Corinth Rift, central Greece. They concluded that signals with a frequency in the order of tens of thousands of years, which is considered high-frequency for that system, were recognisable in the deposits. They also concluded that sediment was building up in the catchment area until it was transported on mass during periods with high amounts of rainfall. Their observations point out that periods of high sediment fluxes leaving the catchment area, sediment input in figure 2, coincide with high discharge and high sediment transport rates.

The distinction between sediment input and diffusivity rate is an important one, since both numerical (Simpson and Castelltort, 2012) and analogue (Van Den Berg Van Saparoea et al., 2008) modelling studies indicate that alluvial systems respond slowly to changes in upstream input flux, but respond quickly to changes in discharge. Naturally the question follows whether this carries over to diffusivity and if so, if differences in discharge are equally sensative to dampening. As to the former, Whipple et al. (1998) linked water discharge to sediment diffusivity in alluvial fans. The latter will be addressed in this research.

The three studies mentioned above do all explicitly point out that the slope of the system is positively correlated to variations in sediment input and inversely correlated to variations in discharge. Thus, when the discharge is decreasing, the corresponding equilibrium slope is increasing, resulting in aggradation of the system and a low sediment output. Conversely, as the discharge is increasing, incision occurs as the equilibrium slope decreases. This eroded material is then transported down the transfer system, resulting in increased sediment output. The reverse is true for the sediment input. It seems therefore, that the discharge may play as significant a role as the sediment input does in generating the transfer system output signal and the sedimentary facies. I suggest that, in order to improve our understanding of the interactions between high-frequency climate cycles and signal recognition in sedimentary deposits, variations in the sediment transport rate should be studied in conjunction with similar variations in the sediment input.

In most diffusion models, including the one used by (Castelltort and Van Den Driessche, 2003), diffusion is kept constant over time. This is, in their words, a 'problem' that 'should be further addressed'. In this research, I intent to address this problem.

1.6 Scaling of synchronous variations

When the system is in equilibrium, the slope, and therefore the sediment flux, is the same across the entire fan. A change in diffusivity would therefore change the sediment flux the same in every location. The topographic profile would thus remain identical, if the sediment input flux were to adjust appropriately. Thus, if the sediment input and the diffusivity vary synchronously, their effect on the equilibrium slope could conceivably cancel out.

Conceptually, the sediment input into the alluvial fan represents the sediment flux at the end of a catchment area. It is reasonable to assume that changes in forcing affecting the catchment area would affect the alluvial fan in a similar manner. However, the effects are unlikely to affect the catchment and fan identically. The alluvial fan is made entirely of sedimentary deposits, whereas the catchment area is made of consolidated rock. This difference may influence several factors such as vegetation cover, permeability and runoff patterns, all of which influence the diffusivity of the system.

Therefore, in this research, multiple scaling ratios will be investigated, and their effects on signal preservation compared.

1.7 Diffusive sediment transport models

Ideally, in order to learn about the major processes that govern the interactions between stratigraphic sequence formation and climate, stratigraphies can be compared to climate data from the time of deposition. Unfortunately, such a comparison requires detailed time labelling of the stratigraphy in question as well as sufficient understanding of the climate and its variations during this time. While such comparisons can be made in areas where the geology and the past climate are well documented, even in such cases the required information is not abundant.

An other way to investigate these processes is to construct analogue and numerical models. The power of such models lies in their ability to simplify the system and vary singular elements at a time. This way, the relative importance of various elements in the system can be assessed, which can lead to insights into large scale dynamics of the system. Model results can be compared to stratigraphies to highlight what patterns might be a result of the modelled processes and what patters are still left unexplained.

Many models describing large scale sediment transport over geologic time have already been created. Most of these models are specifically created with a geologic setting in mind, such as deltas or passive margins (Kenyon and Turcotte, 1985; Rivenaes, 1992; Zhang et al., 2019), foreland basins (Flemings and Jordan, 1989; Sinclair et al., 1991) and alluvial fans (Paola et al., 1992; Marr et al., 2000). All these numerical models are based on diffusion as a mathematical and physical description of sediment transport, as introduced in section 1.3.

Traditionally, these models would lump all sediments into one lithology. These models proved very powerful, for example when studying concepts such as sediment supply and accommodation space creation. However, the inability to model multiple lithologies is rather limiting.

Paola et al. (1992) and Marr et al. (2000) expanded upon this approach by creating two regimes with different diffusivity constants, one representing the transport of gravel and one that of sand. This model assumed perfect sorting, only depositing sand when all gravel was deposited. No mixing of grain sizes in a deposit was allowed. Using this method, Paola et al. (1992) investigated the response of an alluvial basin to various forcing cycles by applying sinusoidal variations to the subsidence rate, sediment input, gravel fraction and sediment diffusion. This approach assumed however, that all gravel would be deposited before any sand would. Such models, where grain sizes are not allowed to exist in the same place, are referred to as perfect sorting models.

Imperfect sorting models have also been developed that still use the diffusion of sediment to represent changes in topography over time (Rivenaes, 1992; Quiquerez et al., 2000). In these models, two or more grain sizes are assigned their own diffusivity value, but are allowed to be deposited at the same location, in varying compositional fractions. This results in stratigraphies with a lot more profundity, which allows for more detailed interpretations. That is not to say that these types of models are necessarily better, more complex models are after all more difficult to interpret. Yet, a model capable of producing more detailed stratigraphy is more suitable when stratigraphic variations as a result of rapidly changing boundary conditions are of importance to the research question.

1.8 Aim

The aim of this project is to asses whether high frequency signals have a reduced chance to be recognisably preserved in the stratigraphic record. More specifically, I will look into what conditions would dampen or delay signals that are carried by the sediment flux through an alluvial fan. The underlying assumption being that the more dampened a signal is, the more poorly it is preserved, the harder it is to relate it to the initial forcing.

To investigate this, a numerical tool is developed to simulate imperfect sediment transport and deposition in an alluvial fan setting. This software is designed to investigate signal preservation by tracking the system output as well as by having a detailed, time stamped stratigraphy and is made open source[1] .

Starting from very simplistic forcing signals, increasingly complex scenarios are compared to each other in order to gain insight in the relation between the duration of a forcing signal and the resulting stratigraphy. These findings will then be applied to a case study in the Pyrenees, northern Spain.

2 Methods

The model here described will be applied to an alluvial fan setting. It will be subject to various forcing frequencies on the sediment input and sediment diffusivity, concurrently. The response of both the alluvial deposits and the sediment efflux at the end of the alluvial fan is tracked, so it can be related to the forcing signals.

[1] https://github.com/tmillenaar/thesis

2.1 Requirements

In order to provide insight into the aim stated above, the model will need to:
- Show the sediment input and output over time
- Keep track of the time of deposition
- Show the stratigraphic evolution by writing stratigraphic output on a regular interval
- Allow a large degree of freedom for specifying the forcing signals

2.2 Columns and the active layer

Diffusive sediment transport models are based on a sediment flux of which the mass is to be conserved (Culling, 1960; Flemings and Jordan, 1989; Sinclair et al., 1991; Paola et al., 1992; Rivenaes, 1992; Zhang et al., 2019). This sediment flux moves sediment from one column to the next, eroding from- or depositing material in each column. Sediment enters the model-space as a flux at the proximal end and leaves the model-space at the distal end (figure 3 and 4).

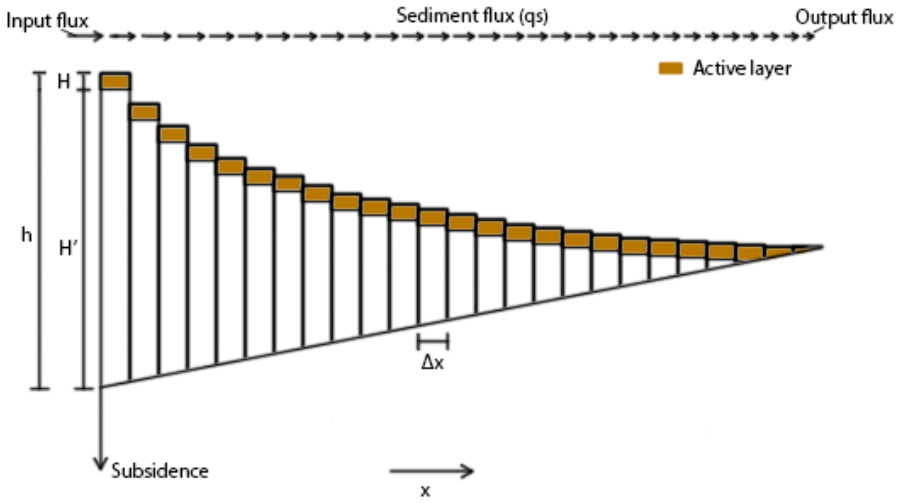

Figure 3: An abstraction of a cross section through an alluvial fan, such as shown in figure 2. Left is the proximal end adjacent to the catchment area, right is the distal end adjacent to the alluvial plane. The sediment flux decreases as the slope decreases.

In perfect sorting, the columns are homogeneous in lithology. One therefore only has to consider the change in height or mass of the column, which is easy to implement and quick to execute. This approach does however not work when imperfect sorting is assumed. Gravel that is covered by a layer of sand, for example, should not be transported to the next column until the overlying sand is removed. To account for this, only the top of each column is considered. This control volume (figure 4) is the area of which the properties are considered during the calculation and on which the flux is applied. It is located at the top of each column. The height of the control volume is the same across all columns and for each iteration in time. It is reduced to the total height of the column in the case that the total height of the column is less then that of the control volumes. Taken together. Within a given iteration in time, dt, this control volume can grow or shrink, after which the height of the control volume is reset for the next iteration. This allows for the erosion of a column form the top down and deposition from the top up, taking into account the local grain size distribution. This setup is visually represented in figure 4.

Each column is divided into cells. Each cell has a grain size distribution which may differ form any other cell. Within the cell, the grain sizes are distributed homogeneously. This is used to store spatial information on the distribution of the grain sizes. A control volume is totally independent of these cells and may span multiple cells, or even some cells and a fraction of another. If a control volume spans a cell and a half, each cell containing x kilos of sand, the control volume will contain 1,5x kilos of sand.

The calculations for the movement of sediment flux between a column and a control volume are identical, save for the constraint that no more material may be removed then is present in the

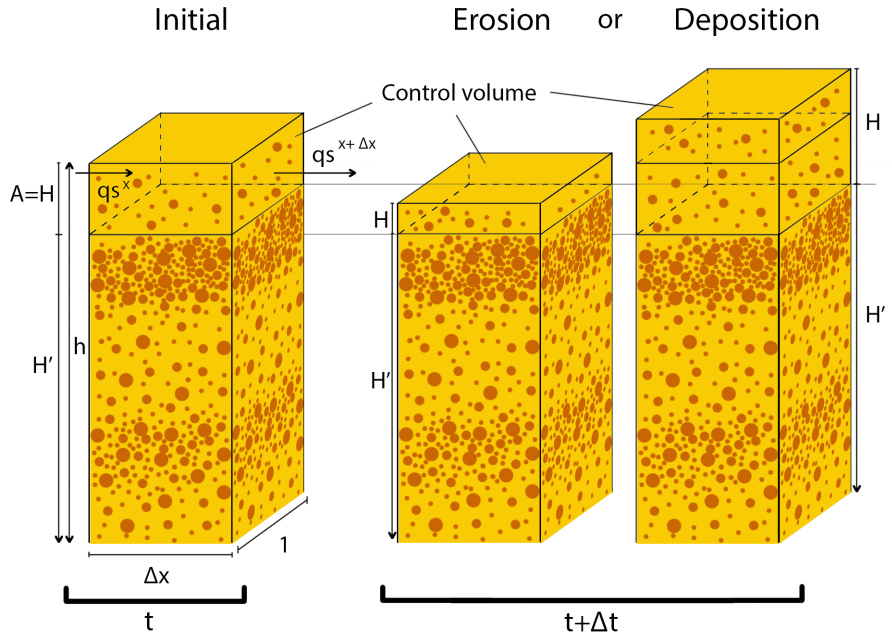

Figure 4: A column containing a control volume is shown. The control volume for the mass balance used in equation 3 is indicated at the top of the column, bounded by H and Δx. A sediment flux (qs) with density ρ_0 passes through the control volume. The total height h is made up of H', which is constant during the iteration and H, which decreases if erosion takes place and increases if deposition takes place.

control volume during any given time step. This is to prevent all of a given grain size to be removed at once from a column, regardless whether this material is located at the top or the bottom.

All control volumes taken together are termed the 'active layer', and represents layer in which sediment is actively transported, see figure 5b. The thickness of the active layer is somewhat arbitrary but should be appropriate for the time scale considered. In this study I use a thickens of 1m, representing the depth of a distributing gully.

To ensure that no more material is eroded then would be present in a control volume, each time step is set dynamically, so that the mass loss in the control volume with the maximum amount of erosion does not exceed the total mass in that volume.

2.3 Sediment flux and Flux fractions

It is assumed in this model that each grain size fraction is transported individually, meaning that the presence of a certain grain size fraction in the sediment flux (qs) does not influence the ability of any other grain size fraction to be transported by said flux. Also, each grain size fraction is assigned an individual diffusivity constant. Conceptually this can be seen as the various grain size fractions having different transport mechanisms, like bed load and suspended load. In order to keep track of the amount of sediment in the sediment flux per grain size fraction, the flux fraction (f) is introduced. Each grain size fraction is given a flux fraction between 0 and 1, which indicates the amount of sediment present in the flux for a particular grain size fraction. Here, 0 indicates that there is no sediment present in the flux of that particular grain size fraction, and 1 means that the sediment flux is saturated for that particular grain size fraction so that no additional sediment of that grain size fraction can be transported. Since material may be deposited or eroded in each control volume, the flux fractions entering a control volume are generally different from the flux fractions leaving that same control volume. Each grain size is considered individually, each having its own diffusivity constant. Consider therefore the sediment flux and the diffusivity to be lists or vectors with a length equal to the number of grain sizes, where each subsequent location represents a different grain size. Any given location j in the diffusivity vector corresponds to the same location j in the sediment flux vector and thus refers to the same grain size. The equation

for the diffusive sediment flux of grain size j is given by:

$$\mathrm{qs}_j = K_j \frac{\delta h}{\delta x} \tag{2}$$

Where qs_j is the sediment flux for a given grain size j in $m^2 s^{-1}$, K_j is the diffusivity constant for that grain size in $m^2\, s^{-1}$, h is the height of the sediment body at that location and x is the horizontal distance from the source, both in m.

In this study, only two grain sizes are considered, gravel and sand. For all practical purposes, one could interpret one diffusivity constant to represent a small variety of grain sizes in that domain. So the sand diffusivity, for example, could represent the transport of medium to coarse sand, as long as they have a shared transport mechanism.

2.4 Diffusion equation derivation

The change of mass in the control volume corresponds to a change in height, see figure 4. The magnitude of these changes is dependent on the length of the time step considered (Δt). The general mass balance in a control volume, during a short time Δt is given by:

$$\begin{gathered} \left[m_{dep}\right]^{t+\Delta t} - \left[m_{dep}\right]^{t} = m^{in} - m^{out} \\ \text{or equivalently} \\ \left[m_{dep}\right]^{t+\Delta t} - \left[m_{dep}\right]^{t} = \left[m_{flux}\right]^{x} - \left[m_{flux}\right]^{x+\Delta x} \end{gathered} \tag{3}$$

Where $\left[m_{dep}\right]^{t}$ refers to the mass of the deposit in the control volume at a given moment in time t and m^{in} and m^{out} represent the mass flux in and out of the control volume, respectively.

The mass of a control volume can be described in terms of its volume and density ($\overline{\rho}_H$). In the same manner, the mass in transport per second at a given location can be described by the transported volume per second times its density. The total sediment volume in transport is simply taken to be the sum of qs for each grain size (j). Assuming there is no compaction, equation 3 becomes:

$$\left[\Delta x\, H\, \overline{\rho}_H\right]^{t+\Delta t} - \left[\Delta x\, H\, \overline{\rho}_H\right]^{t} = \left[\sum_j \left(\mathrm{qs}_j\right) \rho_0 \Delta t\right]^{x} - \left[\sum_j \left(\mathrm{qs}_j\right) \rho_0 \Delta t\right]^{x+\Delta x} \tag{4}$$

Where H is the height up from the initial depth of A at initial time t in m (see figure 4), ρ_0 is the sediment density of both the sediment in flux and any newly deposited sediment in $kg\, m^{-3}$ and $\overline{\rho}_H$ is the average density in height range H in $kg\, m^{-3}$. Since it is already assumed that there is no compaction, if we add the assumption that the density of each grain is the same, regardless of its size, the density never changes. This means that $\overline{\rho}_H = \rho_H = \rho_0$. 4 therefore becomes:

$$\left[\Delta x\, H\right]^{t+\Delta t} - \left[\Delta x\, H\right]^{t} = \left[\sum_j \left(\mathrm{qs}_j\right) \Delta t\right]^{x} - \left[\sum_j \left(\mathrm{qs}_j\right) \Delta t\right]^{x+\Delta x} \tag{5}$$

Divide both sides by $\Delta t \cdot \Delta x$ and let Δt and Δx tend to zero and we get the simplest form of the Exner equation (Paola and Voller, 2005):

$$\frac{\delta H}{\delta t} = -\sum_j \left(\frac{\delta \mathrm{qs}_j}{\delta x}\right) \tag{6}$$

Inserting equation 2 into equation 6 yields:

$$\frac{\delta H}{\delta t} = \sum_j \left(K_j\right) \frac{\delta^2 h}{\delta x^2} \tag{7}$$

The change in height of the control volume during a time step Δt is, by design, also the change in height of the whole column during that time step (see paragraph 2.2 and figure 4). Thus $\delta H = \delta h$ which gives:

$$\frac{\delta H}{\delta t} = \sum_j \left(K_j\right) \frac{\delta^2 H}{\delta x^2} \tag{8}$$

This is the main equation used in this research to describe the diffusion of sediment. It relates the change in height over time ($\frac{\delta H}{\delta t}$) to the overall topographic profile of the fan. If the slope ($\frac{\delta H}{\delta x}$) is the same everywhere, the second derivative of the height ($\frac{\delta^2 H}{\delta x^2}$) is zero and therefore, there is no change in slope over time. A linear topographic profile is therefore the equilibrium condition.

Note that rightward is generally downhill in this setup, which would mathematically be seen as a negative slope. In speech however, a slope is always positive for there is no implied coordinate reference system. So in this case if the slope decreases, or becomes less steep, $\frac{\delta H}{\delta x}$ becomes *less negative* and $\frac{\delta^2 H}{\delta x^2}$ will be positive.

In order to use equation 8 numerically, it can be descretezised using the *Forward Time Central Space* (FTCS) method (Slingerland and Kump, 2011) which yields:

$$H_i^{t+1} = H_i^t + \frac{\sum_j \left(K_j\right)\Delta t}{(\Delta x)^2}\left(H_{i-1}^t - 2H_i^t + H_{i+1}^t\right) \tag{9}$$

This method of discretization brings with it the following condition:

$$\Delta t \leq \frac{\Delta x^2}{2\sum_j \left(K_j\right)} \tag{10}$$

This condition is used to dynamically adjust the size of the time step. Since each grain size has its own maximum Δt as obtained by equation 10, the smallest variant is chosen. Also, Δt is limited by the maximum amount of erodible material in the active layer (recall section 2.2). Again, the smallest Δt is chosen.

Note that equation 9 yields the newly obtained height of the control volume (H). In order to obtain the total height of the column (h), H is to be added to the height of the inactive part of the column, H' (see figure 4).

2.5 Boundary conditions

The part of equation 9 that describes the change in height can be split into two parts, a flux of grain size j into control volume i (Sed_j^{in}) and a flux of grain size j out of control volume i (Sed^{out}):

$$\begin{aligned} \text{Sed}_j^{in} &= \frac{K_j \Delta t}{(\Delta x)^2}\left(H_{i-1}^t - H_i^t\right) \\ &\text{and} \\ \text{Sed}_j^{out} &= \frac{K_j \Delta t}{(\Delta x)^2}\left(H_{i+1}^t - H_i^t\right) \end{aligned} \tag{11}$$

Sediment arriving at the distal end of the model, leaves the modelled space and is considered output. Sediment leaving the fan enters the alluvial plain, which is not part of the modelled space. Sediment output of the modelled alluvial fan is this input for the alluvial plain, just as sediment output of the catchment area is considered input for the fan. The flux out of the distal end is monitored through the Sed_j^{out} term of the second to last column. It is assumed that there are no base level variations. This is implemented by forcing the height of the most distal column to be zero, after Paola et al. (1992). The most proximal column is assigned a sediment flux into the control volume at its surface. These are values that take the place of Sed_j^{in} for the first column. These input flux values, as well as the diffusion coefficients (K_j) and the subsidence, can be specified beforehand to vary through time. Subsidence is implemented as a rigid beam, rotating around a pivot point located at the distal end of the model, also after Paola et al. (1992). For the purposes of this paper, the rotation is conceptually driven by the mass of the overriding plate, visualised in figure 2. When the model is applied at a smaller scale, one could conceptualise it as the movement over a large lystric fault, creating a roll over anticline. The 'subsidence' value assigned in the model represents the subsidence rate at the proximal end of the model, which decreases linearly towards the distal end, where the subsidence is always null.

2.6 Tracking stratigraphy

In order to model a stratigraphy using a discrete method, the modelled volume is divided up in sections. Each column i is divided into individual cells of one metre thick and Δx metres wide. Each cell contains information of its sediment content. A fully filled cell may for example contain 62.3% gravel and 37.7% sand. Within the cell, the grain size distribution is considered to be uniform. When a cell is partially filled, the percentages per grain size will not add up to 100. A cell containing 30.0% gravel and 30.0% sand, for example, would be underfilled and the remaining 40.0% is considered to be empty. This can only happen in cells at the surface.

Each cell also contains a value that represents the last time sediment was deposited in it.

3 Results

The results will be shown for progressively more complicated scenarios. First, the results of a singe forcing pulse will be shown in section 3.1, with the intention of developing some understanding of the basic interactions within a diffusivity driven system. Cyclic variations in forcing signals are explored in 3.2, meant to represent climate fluctuations. A division is made between rapid, high-frequency forcing forcing cycles and long, low-frequency forcing cycles, based on the definition given in section 1.3.

3.1 Pulse signals

First, three scenarios are compared, each with a constant sediment input, except for a sediment input pulse with a duration of 10kyr. The first scenario is one with no subsidence and constant diffusivity (figures 6a and 5a), the second is one with a subsidence rate of 2mm yr^{-1} and constant diffusivity (figures 6b and 5b), and the third run is one with both subsidence and a pulse in diffusivity that is synchronous with the pulse in sediment input (figure 6c).

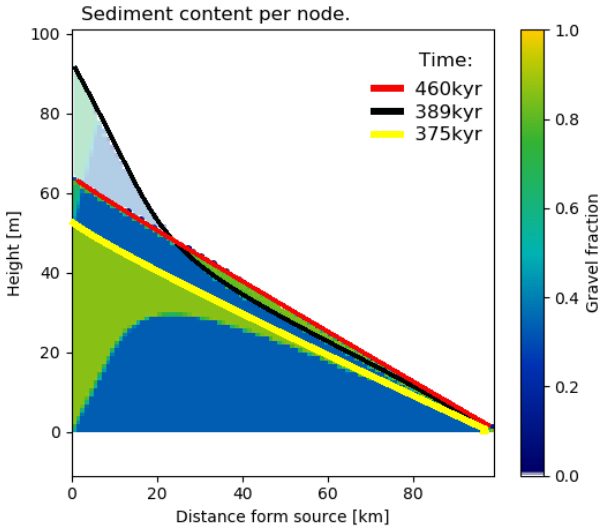

(a) With no subsidence, the eroded pulse material (faded area) is transported as a thin lobe, some of which is found in the green area between the black and red lines, the rest of which already left the system by 460 kyr.

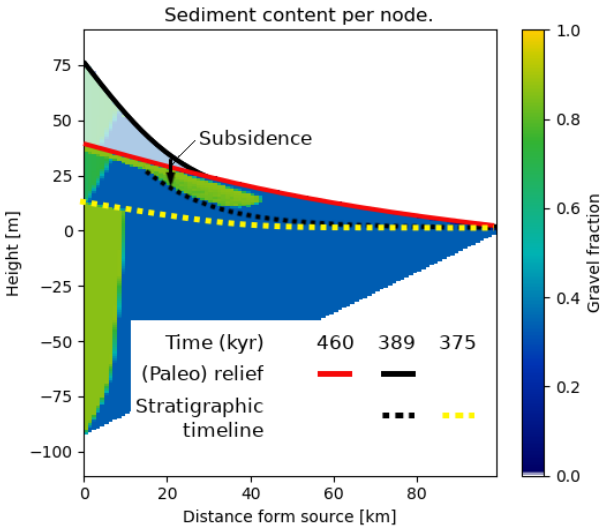

(b) With a subsidence of 2mm yr^{-1}, the eroded pulse material (faded area) is transported as a thicker lobe, which makes it approximately half way down the slope before it is fully incorporated into the stratigraphy due to subsidence and subsequently covered by finer sediments. "(Paleo) relief" indicates the absolute relief at a given time. "Stratigraphic timeline" indicates a line in the stratigraphy that represents a past relief that is now covered, tilted and possibly partially eroded.

Figure 5: Stratigraphic response of the transfer system after a 10kyr lasting pulse of sediment. Corresponding forcing is shown in figures 6a and b. Total elapsed time is from 0 to 470kyr, with the pulse lasting from 380-390kyr.

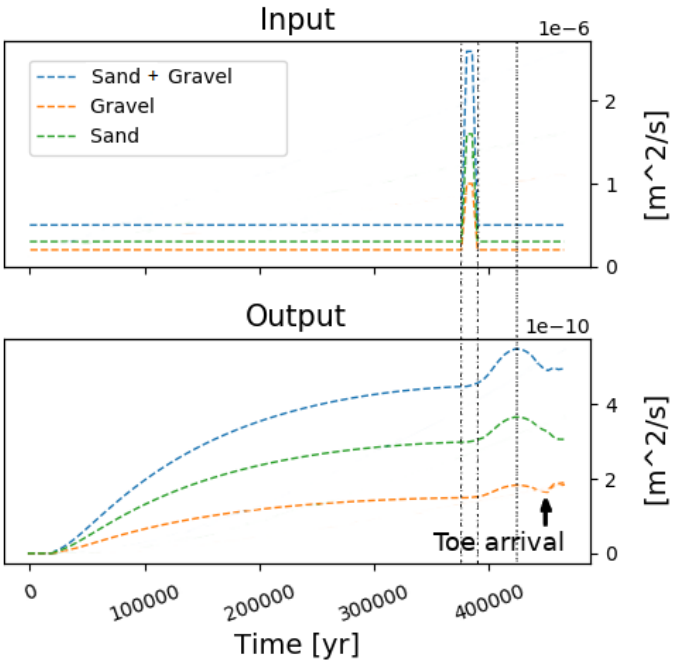

(a) The effect of a sediment input pulse on a system in equilibrium, with no subsidence. "Toe arrival" indicates the moment in time when the front of the lobe, consisting almost entirely of material deposited during the input pulse, reaches the distal end of the transfer system.

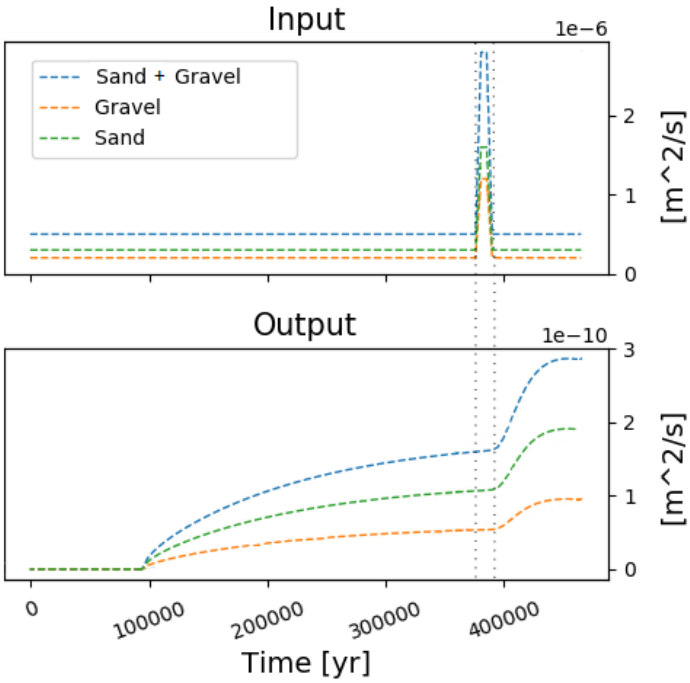

(b) The effect of a sediment input pulse on a system in equilibrium, with a constant subsidence of 2mm yr^{-1}. The diffusivity is a constant 6.4e-4 and 3.2e-4 m^2/s for sand and gravel, respectively. The output signal responds ~4 kyr after the input is returned to its original values. No "toe" or "lobe" arrival is present in this output.

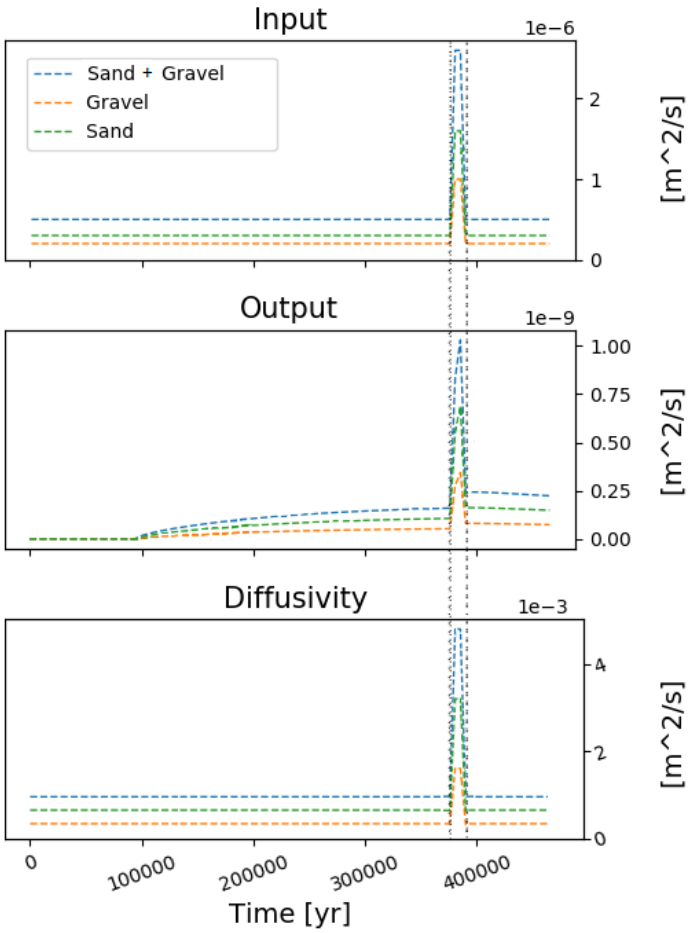

(c) A system in equilibrium with a constant subsidence of 2mm yr^{-1} and a proportionally increased diffusion during the sediment input peak. The output now shows a peak that exactly coincides in time with the input peak and ends as abruptly.

Figure 6: The effect of a 10kyr sediment input pulse on the sediment output of the system. With the exception of the pulse in figure c, the diffusivity is a constant 6.4e-4 and 3.2e-4 m^2/s for sand and gravel, respectively. Note that the output signal responds directly after the input signal is returned to its original values when the diffusivity is kept constant (a, b). When the diffusivity changes along with the input (c), the output is exactly aligned with the pulse.

When there is no accommodation space creation facilitated by subsidence (figure 6a), the signal is highly dampened by the time it arrives at the distal end of the alluvial fan. Even though the total sediment input increased about five fold during the pulse, the total sediment output only increased by about one sixth. The output response was however smeared out over a longer period of time of about 40kyr, as opposed to the 10kyr input pulse. In the case with subsidence (figure 6b), the output response shows a larger increase, and one that is spread over an even longer period of time. Note however that the magnitudes are not the same. The case with subsidence has an overall smaller output flux as a consequence of the continuous accommodation space creation.

During the input pulse, the newly arrived material is accumulating upstream (figure 5a). This upstream accumulation of sediment had a steep linear slope and only starts shrinking once the input is returned to normal. The restored conditions cause the accumulated sediment to move down the slope as a lobe, covering underlying finer grained material (figure 5a). The arrival of this lobe at the distal end of the transfer system can be recognised as an increase in gravel output, marked as 'Toe arrival' in figure 6a. With subsidence, this lobe grinds to a halt and never makes it to the end of the alluvial fan (figure 5b). Instead it is preserved in the fan deposits.

When the diffusivity remains constant, as both in figures 6a and b, the moment the response in the output signal is first visible directly coincides with the moment the input is returned to pre-pulse values. This is not the case in figure 6c, where the diffusivity is increased synchronously with the sediment input. Here, the peak in output corresponds exactly with the peak in input and diffusivity.

3.2 Cyclic signals

3.2.1 Amplitudes and magnitudes

The amplitude of a signal, as well as the relative magnitudes between the input and diffusivity (section 1.6) may be important to the survival of a signal. The results shown in figure 7 are meant to give insight into the importance of the amplitudes. All cycles are simple sine waves with one period of about 60kyr. This period is not intended to represent a specific natural process but is rather a product of convenience. Importantly, the period is well below the equilibrium time of the system. None of the cases in figure 7 have subsidence.

The first two figures (7a and b) have constant diffusivity. Only the sediment input differs, where the latter has a higher amplitude than the former. Figure 7c shows the result of only varying the diffusivity with a constant sediment input. Figures 7d and e are combinations of the first three, where the sediment input and the diffusivity are varied in sync. Again, the latter has a higher sediment input amplitude than the former.

Figures 7a and b show that variations in sediment input result in highly dampened signals in the output of the transfer system, which is consistent with the pulse results and the findings of Castelltort and Van Den Driessche (2003) and Allen (2008). Comparing the output of these two figures shows that the shape and magnitude of the output variance is dependent on the magnitude of the input variance. A low input variance creates mere bumps in the output signal, whereas a high input variance results in a highly asymmetric output response. The delay is also slightly different, with a ∼27 kyr delay in figure 7b and a ∼33 kyr delay in figure 7a. The diffusion on the other hand (figure 7c), has a very direct impact on the output of the transfer system. The diffusion and transfer system output have a very correlatable graph shape, though the becomes smaller as the system approaches its equilibrium slope. When the system is at its equilibrium slope, the response of the output to variations in diffusivity is near instantaneous.

Moreover, the diffusivity seems to be dominant over the input signal when it comes to the shape of the output signal. In fact, the difference can be so stark that the delayed response caused by the input variations is nearly, if not completely masked by the diffusivity variations when both parameters are varied simultaneously (figure 7d). A delayed response to a high input signal however, can prevent some of the decrease in the transfer system output in periods of low discharge (figure 7e).

3.2.2 High-frequency cycles

In the stratigraphy of the fan, very high frequency forcing variations tend to create sand rich strata at the distal end of the transfer system (figure 8). Whether these strata correspond to maximal

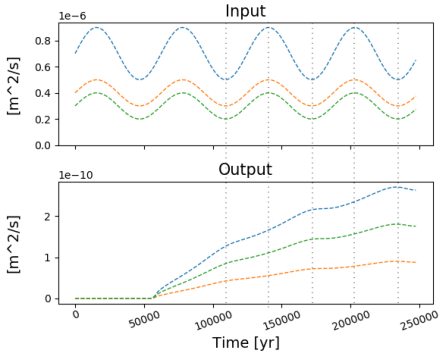

(a) Low input variations. Diffusivities are a constant 3.2e-4 and 6.4e-4 m^2s^{-1} for gravel and sand, respectively.

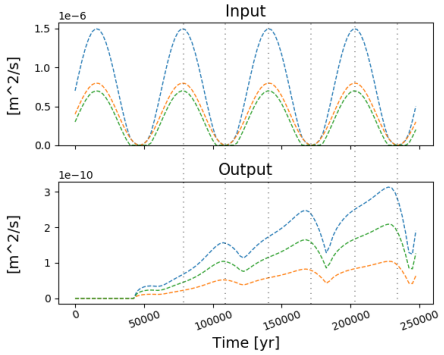

(b) High input variations. Diffusivities are a constant 3.2e-4 and 6.4e-4 m^2s^{-1} for gravel and sand, respectively.

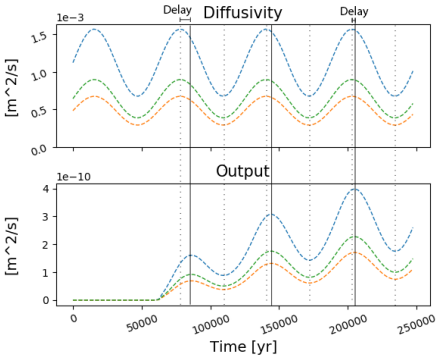

(c) Diffusion variations. Input fluxes are 4e-7 and 3e-7 m^2s^{-1} for gravel and sand, respectively.

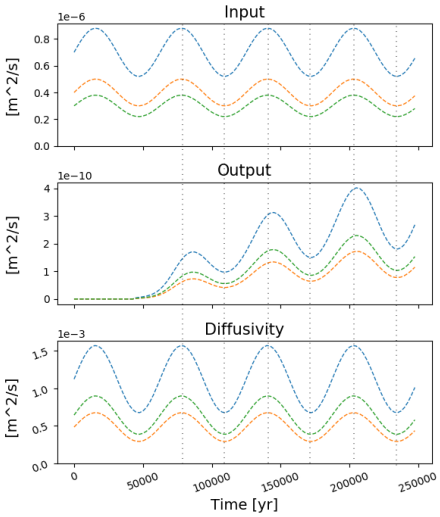

(d) Both diffusion and low input variations in sync

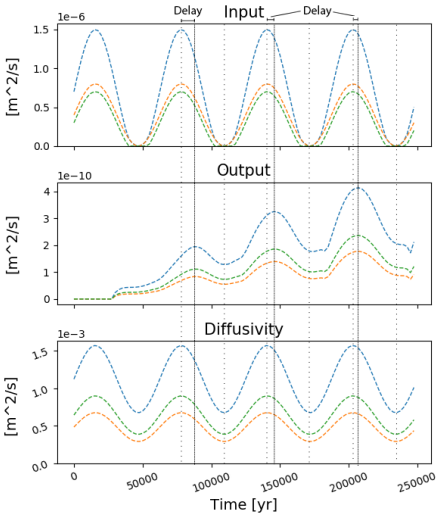

(e) Both diffusion and high input variations in sync

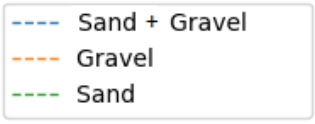

(f) Legend

Figure 7: The effect of input and diffusivity variations on the output of the transfer system. None have no subsidence.

retreat or maximal propagation of the gravel front, depends on the relative rate of increase in sediment input and diffusion. In the case of a high sediment input variation (figure 8a), two different laterally correlatable facies are deposited during the lows in forcing. In the proximal end of the basin, a gravel-rich layer is developed that retreats as swiftly as it propagates, resulting in a well recognisable gravel spike in the stratigraphy. At its head, this spike abruptly transitions into a synchronously deposited, sand-rich layer that extends the rest of the profile to the distal end. In the scenario of an identical setup, but with a lower input variation (figure 8b), the lateral correlation between distal sand-rich layers and the propagation of the gravel front is inverse. Here, the distal sand layers correspond to a rapid maximal retreat of the gravel front instead of a maximal propagation. In both cases, the distal sand strata are formed during lows in the forcing cycles, but the timing of gravel front propagation is different. During high input variations, maximal gravel front propagations coincide with maxima in forcing, whereas they coincide with minima in forcing during low input variations.

If the variations in both the input and diffusion are small (figure 9a), no rapid gravel front propagations occur, given the subsidence rate is large enough. Also, the extra coarse beds do not form, leaving the proximal deposits to be rather uniform in its sorting. In an identical case, but with a higher sediment input variation (figure 9b), the extra coarse beds do form, even when the diffusion is kept constant (figure 9c). For the creation of periodic coarse beds, variations in diffusivity are not required, a constant difference in diffusivity between the grain size regimes is sufficient, given there is an alternation between periods of low and high sediment input. The formation of the coarse beds coincides with lows in input in both figures 9b and c. Periods of low input also allow for propagation of the gravel front.

Distal sand rich layers form even when both variations in sediment input and diffusion are small (figure 9b). It appears that a small variation in diffusivity is already capable of creating alternating

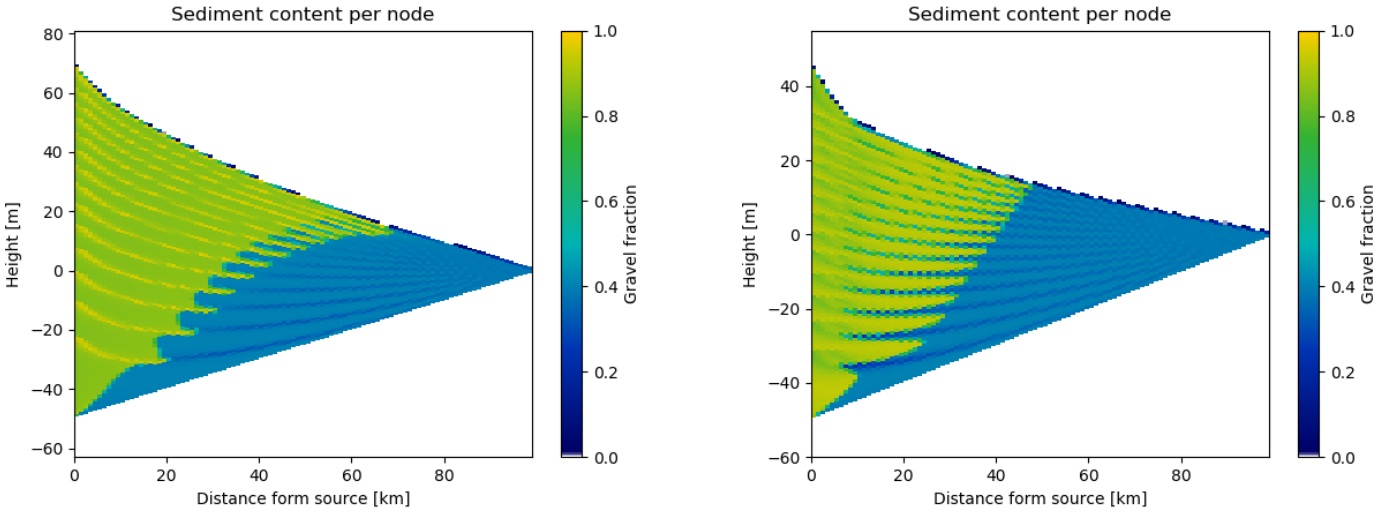

(a) High input amplitude

(b) Low input amplitude

Figure 8: Transfer system stratigraphy resulting from rapid high-amplitude forcing changes with a subsidence rate of 2mm yr^{-1}. The corresponding forcing and transfer system output are shown in figure 13 in appendix A.

sand saturations in the intermediate to distal end of the model. A fully constant diffusivity creates a fully uniform distal facies with no alternating sand saturations (figure 9c). This implies that variations in proximal sediment input have barely any influence on the distal facies in a large transfer system.

The angle at which the gravel front is propagating, either for periods of constant forcing or the average of multiple rapid oscillations, is determined by the total volume balance. This total volume balance is made up of input, output and accommodation space. If the subsidence rate is high enough to create enough accommodation space for most gravel to be stored, the gravel front variations oscillate around the same distance from the source (figure 9). A consistently low subsidence rate however, results in a constantly propagating gravel front, averaged out over a period (figure 8).

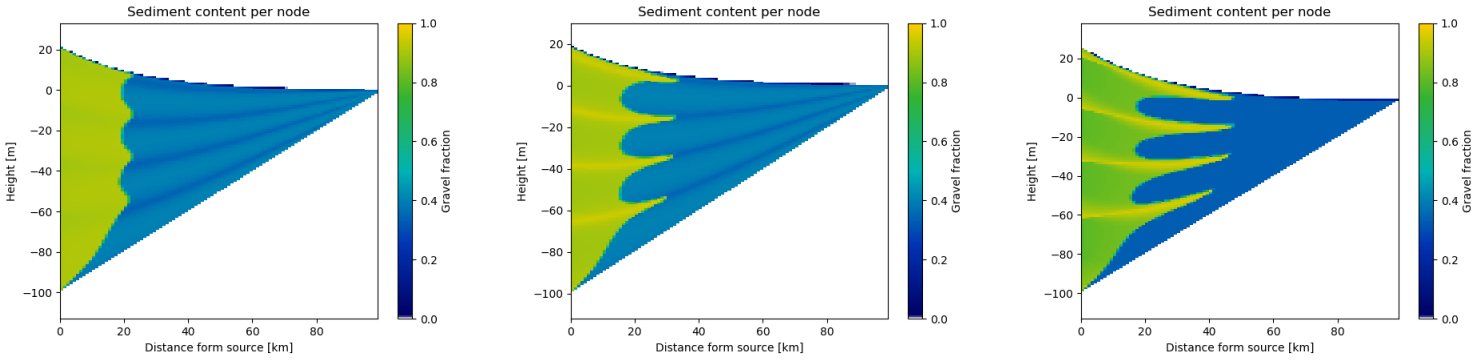

(a) Low input amplitude

(b) High input amplitude

(c) High input amplitude, no diffusion variation

Figure 9: High-frequency transfer system deposits showing different styles in gravel front variation through time for different forcing scenarios. These scenarios contain 4 cycles, ∼62 kyr each, spanning ∼250 kyr with a constant subsidence rate of 4mm yr^{-1}. For forcing corresponding to these results, see figure 14 in appendix A.

3.2.3 Long forcing cycles

So far, mostly rapid ($< T_{eq}$) changes have been discussed. The output signal is very predictable for it follows the forcing, especially the diffusion variations, very closely (see figure 15). The obvious exception is when the basin is underfilled, for the excess accommodation space will need to be filled before the system yields output. This scenario happens mostly in the lows of long input variations, when a long period of low input cannot keep up with the accommodation space creation facilitated by the constant background subsidence. It turns out however, that transfer system deposits resulting from slow forcing variations are quite different then those resulting from rapid forcing variations.

Upon investigation of the results shown in figure 10, one of the first things one may observe is the rather whimsical gravel front alternation within a given period. This whimsical pattern does repeat every cycle however, suggesting there is a method to the madness.

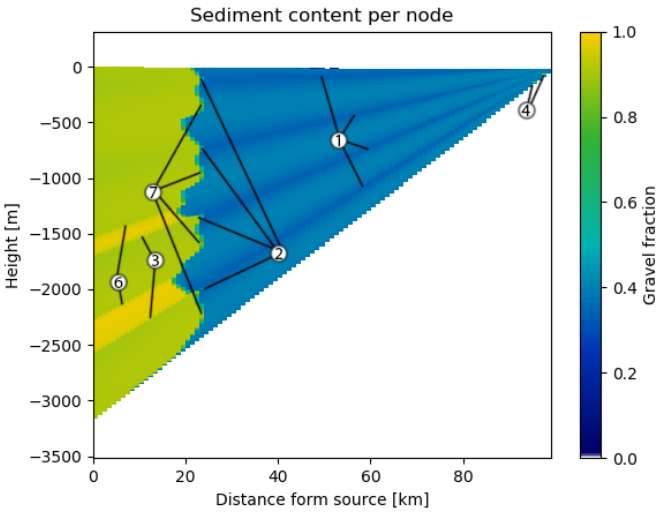

(a) Low input amplitude for ∼8 myr

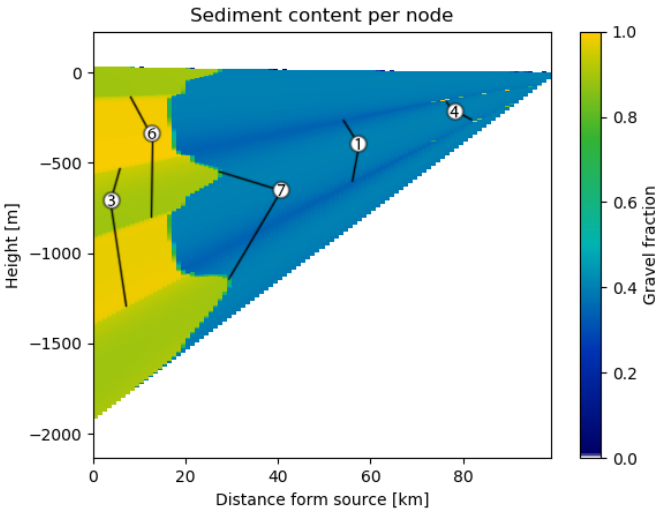

(b) High input amplitude for ∼5 myr

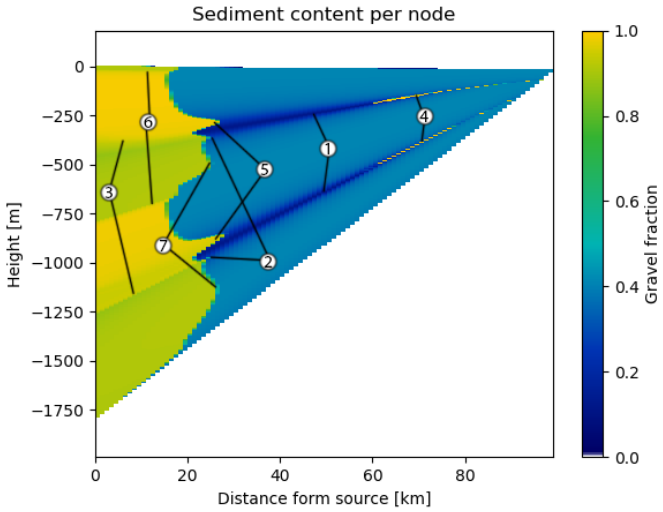

(c) High input amplitude and high diffusion amplitude for ∼5 myr

Figure 10: Low-frequency, 2 myr period, transfer system deposits showing different styles in gravel front variation through time for different sediment input amplitudes. For forcing corresponding to these results, see figure 15 in appendix A.

It was established in the previous section, that diffusivity changes result in the periodic appearance of sand beds in the more distal, sand dominated domain. Also here, lows in diffusivity create these recognisable layers where the middle of the sand layer corresponds the the minimum in diffusivity ①. Around this time, the lows in sediment input cause the gravel front to propagate ever so slightly ②. These moments of minima in the forcing cycles correspond roughly, though not exactly, to the onset of an episode where proximally extremely sand-poor deposits are formed. The onset of this episode is instead directly linked to the moment the basin becomes underfilled ③. Even in periods of rapidly increasing sediment input, as long as the basin is underfilled, the deposits created during that time are extremely sand-poor in the coarse, proximal regime. While the reason is not clear to me as of yet, it seems that the presence of excess accommodation space promotes the drainage of sand from the proximal gravel regime.

Underfilled episodes are longer if the input variation is larger, for lower frequency variations result in longer stretches of time where accommodation space creation through subsidence goes uncontested. The longer episodes of high input do not compensate for this, for (1 the depression created during the previous low in input must be filled and (2 excess material during highs in sediment input leaves the system at the distal end.

Long episodes of low input create valleys so that the lowest topography is not in the distal end of the model. In such cases, the diffusivity in the very distal end of the model is negative, which causes sediment to flow back. Sand is therefore drained from the distal part of the model and transported to intermediate locations where the low in topography resides, resulting in very thin distal gravel beds ④. This scenario assumes sediment transport from the distal end of the model back to the intermediate topographic low with the same slope dependent rate as the forward sediment transport. The realism of this scenario is highly debatable, but one could imagine a flexural ride from where material is transported down slope into the foreland basin.

If the diffusivity was extremely low during the low in forcing, but some sediment was still coming into the basin, the eventual increase in diffusivity transports the build up material further into the basin. This can create a spike in the gravel front ⑤, the extent of which is mostly determined by the amount of proximally stored material, the accommodation rate creation and ultimately the location of the current low in topography.

As sediment input increases, the excess accommodation space starts to fill. As soon as the basin relief is fully above base level, the gravel fraction for the proximal regime is returned to its original value range ⑥. From here the system keeps building up and outward, until the sediment input is again too low to keep up with the accommodation space creation. When the accommodation space creation is larger then the input, the gravel front retreats again. The furthest gravel front location from the source therefore corresponds with the highest relief ⑦.

Upon even closer inspection, more nuances can be pointed out. This highlights the intricacy of a system where sediment input and transport vary together in sync.

4 Discussion

4.1 The equilibrium slope: erosion or deposition

When the boundary conditions change, the equilibrium slope changes as well. This is perhaps most evident in figure 5a. Here, a sediment body is growing at the proximal end of the model, the accommodation space for which is facilitated by the increase in equilibrium slope as a result of the increased input.This proximal sediment body displays the new, steeper equilibrium. The difference between the old and new equilibrium slope can be seen in the black line. The fan would keep growing until the whole fan reaches this slope, were it not for the reduction in equilibrium slope after the input flux returned to normal.

This figure also showcases how a reduction in equilibrium slope facilitates erosion. Left of the intersection between the red and black lines, material has been eroded until the slope reached the red line, approximately the equilibrium slope for the set conditions. Where the steepness of the local slope exceeds that of the equilibrium slope, the sediment flux is higher then the input flux, thus resulting in a reduction of the slope until the local slope equals the equilibrium slope. The eroded material is deposited in locations where the local slope is lower then the equilibrium slope, see the green between the red and black lines, to the right of their intersection. Any eroded material not stored below the equilibrium line is transported out of the model-space, onto the alluvial plane.

Erosion caused by the lowering of the equilibrium slope causes a direct response in the output, see figures **??** and b. Importantly therefore, sediment output of the fan increases when sediment input decreases. This is counter intuitive. In fact, it may be counter intuitive because generally, when the input is low, diffusion is also low, and low diffusion results in low output.

4.2 Gravel beds and the gravel front

The direction of movement of the gravel front is inversely dependent on the change in equilibrium slope. The gravel front propagates or retreats depending on whether the equilibrium slope decreases or increases, respectively. Since the equilibrium slope is positively correlated to the sediment input and inversely correlated to the diffusion rate (Van Den Berg Van Saparoea et al., 2008; Simpson and Castelltort, 2012), the relative rate of change between the sediment input and diffusion variations determines the change in equilibrium slope and, by extension, propagation of the gravel front.

Whether the input or diffusivity controls the change in equilibrium slope, depends on their respective rates of change, as introduced in section 1.3. In the case of highly varying input, the input changes control the change in equilibrium slope. Conversely, the diffusion variations control the change in equilibrium slope when input variations are low.

4.2.1 Input dominated equilibrium slope

In periods where sediment input increases rapidly, the equilibrium slope increases, aggradation occurs and the gravel front retreats. As the sediment input decreases from there, the equilibrium slope decreases and the gravel front propagates. The lows in forcing therefore correspond to maximal propagation of the gravel front. When the decrease in sediment input has reached the point where considerably less material arrives then is transported, the surface layer is depleted of sand, which, along with newly arriving sand, is distributed over the more distal areas of the basin. The result is quite a sharp surge in the gravel front, of which the extend is severely limited by the decreasing diffusion during its propagation, but is laterally correlatable to the more distal sand layer (figure 8a).

4.2.2 Diffusion dominated equilibrium slope

When the rate of change in the diffusion is dominant over the rate of change in the input flux, periods of low diffusion result in a body of coarse material building up at the proximal end of the basin (figure 8b). During this buildup, only fine grained material is transported further into the basin. This results in a very proximally positioned gravel front with a steep slope and a sand rich layer covering the rest of the basin. In periods of high diffusion, the body of coarse material is transported down into the basin, which is why the point of maximal propagation in this case coincides with a maximum in forcing. This is seen in the stratigraphy as a thick, coarse body of sediment, contained at the top and bottom by a sand-rich layer.

4.2.3 Gravel beds

When sediment input is low compared to the diffusivity, gravel beds form on the proximal side of the gravel front (figures 8 and 9). These beds are formed by the drainage of sand from these layers, as a result of the difference in diffusivity between the grain sizes. The larger the difference, the quicker the sand will be drained from the beds.

These beds form mostly when the input is low, for there is time for the difference in diffusivity between gravel and sand to drain sand from proximal deposits. When the input is higher, the constant supply of new material covers the slightly older sediments thus preventing further separation. The amount of sand drainage from a deposit then is dependent on (1 the difference between the diffusivities of the sand and gravel in the system and (2 the rate at which material arrives to bury the sediment at the surface and thereby shelter it from further erosion.

Since both gravel front propagation and the drainage of sand from surface deposits are largely facilitated by lows in sediment input, coarse beds extending far into the basin are not uncommonly produced by the model.

4.3 Response to peaks in precipitation

In moments of increasing precipitation, higher discharge results in deeper channel incision and increased erosion of the catchment area. This newly eroded material is directly transported downstream, which results in rapid gravel propagation and the development of proximal unconformities, as concluded by Paola et al. (1992). The amount of sediment leaving the catchment area during periods of high discharge could be significantly increased by the possible presence of previously weathered, but as of yet untransported material in the catchment area (Watkins et al., 2018). Concurrent with the propagation of the gravel front, as a direct response to the increased discharge, material at all other surface locations in the transfer system is also transported downstream at an increased rate. This results in a near immediate peak in the output of the transfer system, which at first reflects the arrival of already nearby material. The freshly eroded sediment however, arrives at the distal end of the transfer system with a delay, as put forward by Castelltort and Van Den Driessche (2003); Allen (2008). Since material is already arriving at the distal end of the model at an increased rate, the arrival of this recently eroded material may be difficult to recognise in the output signal. Possible changes in average grain size in the newly eroded material are unlikely to make it to, and be recognisable in, the transfer system output. With some luck however, the pulse composition differs from that of previously eroded material as a consequence of the deeper incisions, allowing the pulse material to be traced. Unfortunately this is the exception, not the rule. While the delayed arrival of the input pulse at the distal end of the transfer system may be obscured, the output signal does, in such a case, directly represent the change in climatic forcing.

4.4 Response to lows in precipitation

During times of low deposition, material currently in the active layer is not being covered or diluted with newly arriving material. This gives it it time to propagate and separate. The separation occurs because sand, having a higher diffusivity then the gravel, is drained out of the already coarse proximal deposits. This effect can be amplified if the new climate brings an increased difference in transport rate between the coarse and the fine material. Sand is then drained from proximal deposits even more efficiently. This drained sand is, along with any newly arriving sand, deposited at more distal locations, where layers of sand are formed (figure 8). This tends to create thin beds of coarse material that protect the underlying, more sand-rich deposits, from also being drained of sand. These coarse beds are covered when the sediment input starts to ramp up again. This increased sorting and the possible erosional surface in the transfer system deposits therefore mark lows in sediment deposition.

4.5 High input but low diffusivity

The response to changes in climate forcing of the transfer stratigraphy and output is different when increased sediment input into the transfer does not coincide with a significant increase in discharge. Think, for example of (1 a period rapid uplift of the catchment area or (2 through the release of stored weathered material, induced by a very short or small increase in catchment precipitation. In such a scenario, the increase in equilibrium slope as a result of the increased sediment input trumps the decrease in equilibrium slope as a result of the increase in sediment transport rate. Newly arriving sediment will then be stored in very proximal locations in the transfer system. It is only when the discharge sufficiently increases to also cause significant increases in sediment transport rate, or when the sediment input rate is returned to its original values, that the now proximally stored mass is transported further down. It is around this point that the transfer system output signal may start to show deviations, as increased sediment transport more efficiently transports already distal deposits which can directly leave the system. This effect is enhanced by the now lowered equilibrium slope. The body of eroded proximal material, deposited during the period of increased sediment input, takes the form of a lobe sliding down the transfer system. This leaves an erosive mark in the proximal end of the transfer system and creates a large propagation of the gravel front. The speed of the lobe is partially determined by the subsidence rate which, if large enough, will cause the lobe to come to a halt, leaving a very recognisable impression in the transfer system stratigraphy (figure 5b).

4.6 Storage and release

In some sense, transfer systems as discussed in this paper act as a giant capacitor for sediment. Sediment can enter the system where it can either be released directly or stored for potential later release. The amount of newly stored sediment is then governed by the sediment input and accommodation space creation whereas the release is governed by the sediment transport rate and reductions in accommodation space. Accommodation space is, however, not solely determined by subsidence and uplift, but also by changes in the equilibrium slope as well as base level variations. The equilibrium slope is a complicating factor, for it is dependent on the balance between sediment input and transport rate and is a main focus of this study .

4.7 Shortcomings

Given how the model treats sediment transport as an average over a time period Δt, many high resolution phenomena can not be investigated or even taken into account in this model. It is however a powerful tool when investigating intermediate to long term changes in an alluvial fan. Even so, many features are not implemented that could be of interest to stratigraphers interested in this time frame. Such processes include but are not limited to: compaction, abrasion, composition driven changes in diffusion and base level changes. Further research could investigate the relevance on such parameters on the way forcing signals are processed by a sediment transfer system.

Several studies have, in particular, already investigated base level variations through the use of a sediment diffusion model (Kenyon and Turcotte, 1985; Rivenaes, 1992, 1997; Zhang et al., 2019) and its addition to the model would improve its utility. However, base level variations are not a factor in most alluvial fan settings and it would complicate the dynamics of the system to a point beyond the scope of this research. Nevertheless, I do acknowledge that base level variations play a major role in the general development of alluvial systems.

5 A case study: the Paleocene-Eocene Thermal Maximum

5.1 Introduction

The Paleocene-Eocene Thermal Maximum (PETM) was a brief period, about 58.8 ma (Wing et al., 2005; Zachos et al., 2005), in which greenhouse gasses spiked. In the stratigraphic record, this period is often recognisable by a negative excursion in the δ^{13}C isotopes. During the PETM, sea surface temperatures rose by about 8°-10°C at the poles and by about 5°C at the tropics (Zachos et al., 2003). The oceans acidified (Zachos et al., 2005) and many benthic foraminifera went extinct (Kennett and Stott, 1991). On land, terrestrial plant ranges shifted (Wing et al., 2005) and mammalian species migrated (Bowen et al., 2002). The initial effects of the PETM were firmly established within 10.000 years (Kennett and Stott, 1991; Wing et al., 2005; Zachos et al., 2005) and the whole of the PETM lasted for around 170 thousand (Röhl et al., 2007) to 200 thousand (Westerhold et al., 2017) years.

Subtropical regions in the late Paleocene typically were sparsely vegetated due to high temperatures and seasonal precipitation with dry periods (Schmitz and Pujalte, 2003; Foreman et al., 2012; Foreman, 2014; Kraus et al., 2015). During the PETM, the intensity of the seasonal precipitation in subtropical regions increased and, facilitated by the lack of vegetation, resulted in increases in valley incision, channel width, flooding, channel avulsion and overall weathering (Schmitz and Pujalte, 2003; Foreman et al., 2012; Clechenko et al., 2007).

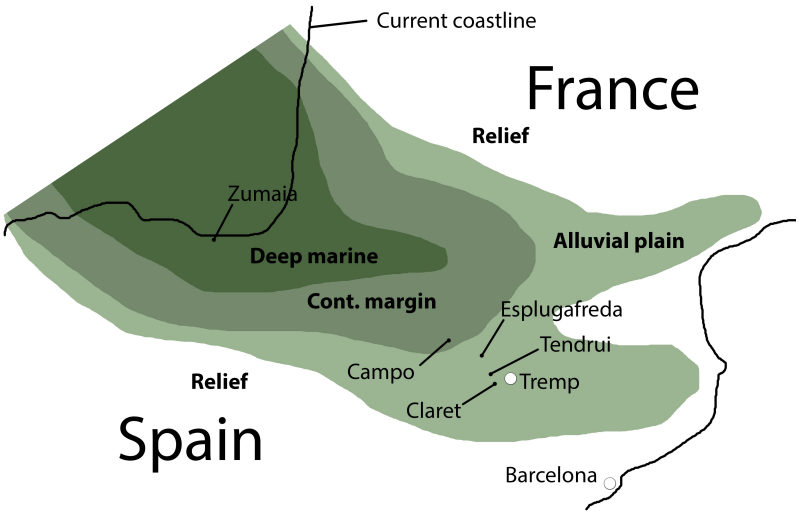

Figure 11: The location of the sites mentioned in this study. Modified after Manners et al. (2013) and Duller et al. (2019). For the corresponding logs, see figures 16 and 17 in appendix A.

The effect of the PETM on the stratigraphic record has been studied in-depth in the Tremp-Graus basin in northern Spain (Schmitz and Pujalte, 2007; Duller et al., 2019). Within about 10kyr, the Tremp-Graus basin developed an extensive braid plane, now recognizable as a 1-4 metres thick, clast supported conglomerate with rounded boulders (Schmitz and Pujalte, 2007). It extends laterally throughout most of the basin and is overlain by fine-grained soils (Schmitz and Pujalte, 2003, 2007). The time of deposition is however not the same throughout the basin. Several studies show a delay between the δ^{13}C excursion and the deposition of the conglomerate (Domingo et al., 2009; Manners et al., 2013; Duller et al., 2019). Comparing the delays of individual sites show that this delay is asynchronous across the basin, increasing for more distal areas (Manners et al., 2013; Duller et al., 2019).

The locations of the sites used in Manners et al. (2013) and Duller et al. (2019) are shown in figure 11. For their respective logs, the reader is referred to figures 17 and **??** in appendix A, respectively.

Duller et al. (2019) estimated the time delay per site based on average sedimentation rates, ranging from a 9-16 kyr delay in the middle of the alluvial plain (Claret section) to a 20-36 kyr delay near the paleo-coast (Campo section) with a 13-24 kyr delay in between (Tendrui section). The Esplugafreda section is an outlier, in that it has next to no delay between the δ^{13}C excursion and conglomerate deposition. It may not be entirely representable due to the slow sedimentation rate of 0.1 m yr^{1} (Duller et al., 2019) and the possible removal of underlying strata through scouring during conglomerate deposition (Manners et al., 2013). This porpagational response does however not extend to the deep marine section of Zumaia. Here, Paleocene carbonates are covered with the so called "Siliciclastic Unit", of which the onset directly coincides with the δ^{13}C excursion (Manners et al., 2013; Duller et al., 2019). A compositional analysis of the Zumaia section, provided by Duller et al. (2019), shows a split reaction to the δ^{13}C excursion. First, the δ^{13}C excursion directly coincides with a rapid increase in the deposition of detrital material. This rapid increase is followed by an even larger increase, separated by about 10 kyr of roughly constant detrital deposition. Duller et al. (2019) attribute the initial increase to the increased discharge affecting the "advective length" (Ganti et al., 2014) of the sediment, which is a measure of the lateral distance sediment is transported before it settles. The second increase occurs 15-18 kyr after the δ^{13}C excursion. They ascribe the delays to an adjustment of the transport slopes to the increased transport capacity.

A very similar stratigraphic marine response is provided by John et al. (2012) for a continental margin setting at the east coast of North America. They plot the kaolinite over smectite ratio (K/S), short term (<1 myr) increases in which they attribute to increased physical weathering on land. A sharp increase in K/S is found 40cm below the δ^{13}C excursion, form which they conclude that both proxies K/S and δ^{13}C have a reliance on similar forcing. At 3.2m above the onset of the deep marine δ^{13}C excursion, K/S shows a second rapid increase, after which it gradually declines.

5.2 An investigation

The results shown earlier in this paper indicate that a rapid gravel excursion can occur in two instances (1 during a decisive low in sediment input as shown in figure 8a or (2 during a decrease in equilibrium slope. The latter can occur during a rapidly decreasing input, possibly combined with a modestly decreasing sediment transport rate shown in figures 9b,c, or during a rapid increase in sediment transport rate, possibly combined with a modest but limited increase in sediment input as shown in figure 8b).

Given the numerous observations indicating increased precipitation and discharge during this period (Schmitz and Pujalte, 2003; Foreman et al., 2012; Clechenko et al., 2007), it seems very likely that the sediment flux from the catchment area to the transfer system was high. Thus, since there was likely no lack of sediment input, option (1 is ruled out.

Various possible instances for option (2 were tried in the model, in an attempt to replicate the scenario. Based on the data of Manners et al. (2013) and Duller et al. (2019), the model results should show a two-step increase in the transfer system output. After this increase, the transfer system output should remain somewhat constant. The results should also show a thin, coarse layer propagating right after the onset of the PETM. This thin layer should be covered by finer material. In Tendrui, this finer material is in turn quickly covered by coarse material, while the other terrestrial sites continue to deposit fine material throughout the PETM. Unfortunately, such three dimensional local variance can not be replicated in the model. Two of the more successful scenarios are shown in the following section.

5.3 Case study results

The double increase in sediment output, visible in the data of both John et al. (2012) and Duller et al. (2019) can be recreated nicely. The first increase is created by a rapid increase in diffusivity. Congruently, the sediment input into the transfer system is increased rapidly. This new sediment arrives at the distal end of the transfer system with a delay, resulting in the second increase.

Concerning the gravel front propagation, two scenarios are investigated. The first, shown in figure 12a, is a result of a sediment transport dominated equilibrium slope adjustment. Both the sediment input and the sediment transport rate are increased significantly, but the increase in sediment transport rate is high enough to propagate the gravel front. This propagation is very short lived however, for it is not the resulting high transport rates that facilitate the propagation but the increase itself, which only spans a few thousand years. This very rapid but short lived ∼8kyr propagation in the gravel front creates a very thin (∼5m thick) coarse layer which is evenly spread over a large part of the basin. Since the sediment input during the PETM is significantly larger then the accommodation space creation can accommodate, the gravel front inevitably propagates when the system reaches its equilibrium slope.

The second scenario, shown in figure 12b, shows the gravel front propagation after the termination of an input pulse. The rationale here revolves around the catchment area. During the dry period preceding the PETM, the catchment area may have been subject to weathering and some local sediment rearrangements, but the bulk of this material may not have been transported to the transfer system due to a lack of discharge. At the onset of the PETM, a sudden increase in discharge may have moved these stored sediments to the transfer system. After this stored material was removed, the sediment input into the transfer system would plummet. During the PETM, the sediment input would however still be significantly higher then before then it was onset of the PETM, for precipitation rates are still high.

The sudden increase in sediment input results in a retreat of the gravel front, which is then followed by a significant advancement of the gravel front as the sediment input decreases again. The coarse layer created in this scenario is significantly thicker then in the previous scenario, exceeding 50m in some locations. This does not match the ∼4m thick deposits found in the Tremp basin. While the input parameters are not confined well enough to properly compare the thicknesses, an order of magnitude difference is rather large. The total propagation time of ∼30kyr is however within the same order of magnitude as the estimated delay times suggested by Duller et al. (2019).

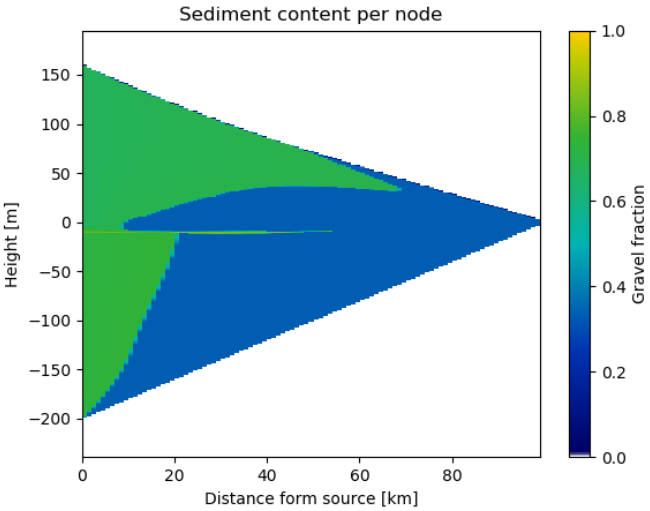

(a) A 1-5m thick coarse bed was deposited directly after the initial increase in sediment transport rate, covered by a thick body of sand. During the PETM, a second, larger body of coarse material is deposited.

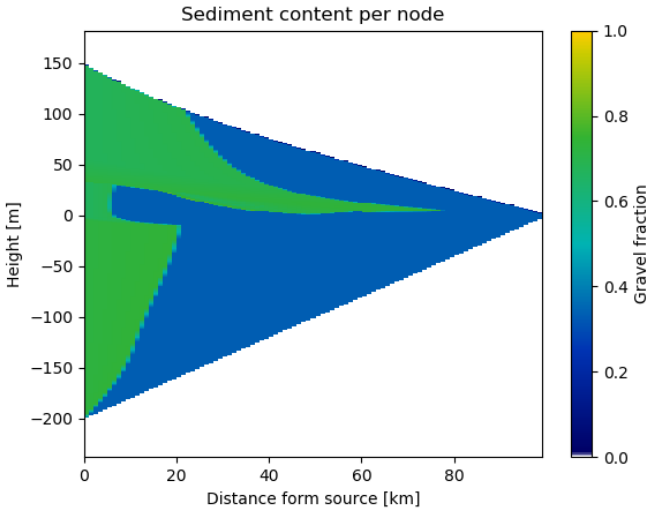

(b) A 1-50m thick bed of coarse material, covered by sand rich deposits.

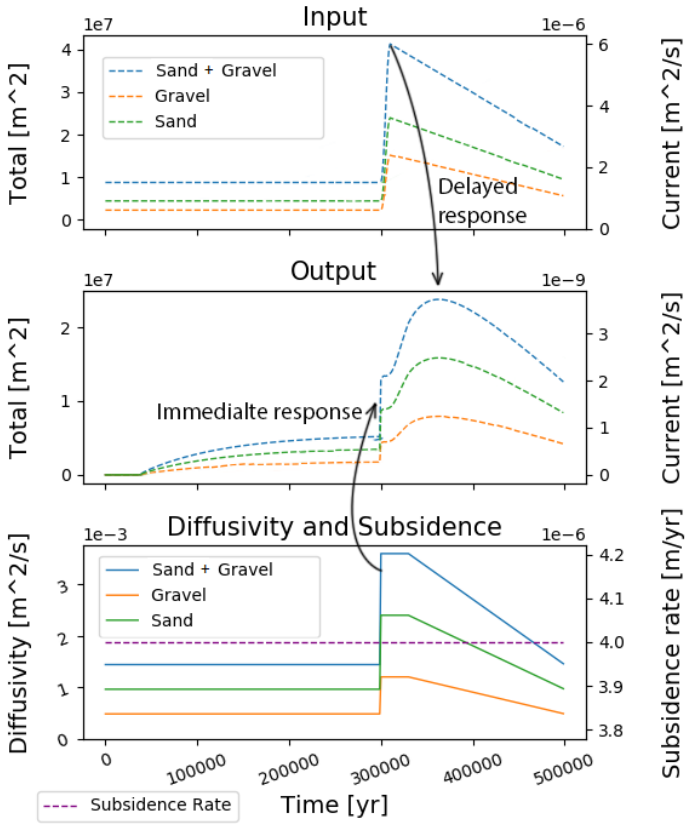

(c) Forcing and transfer system output corresponding to (a)

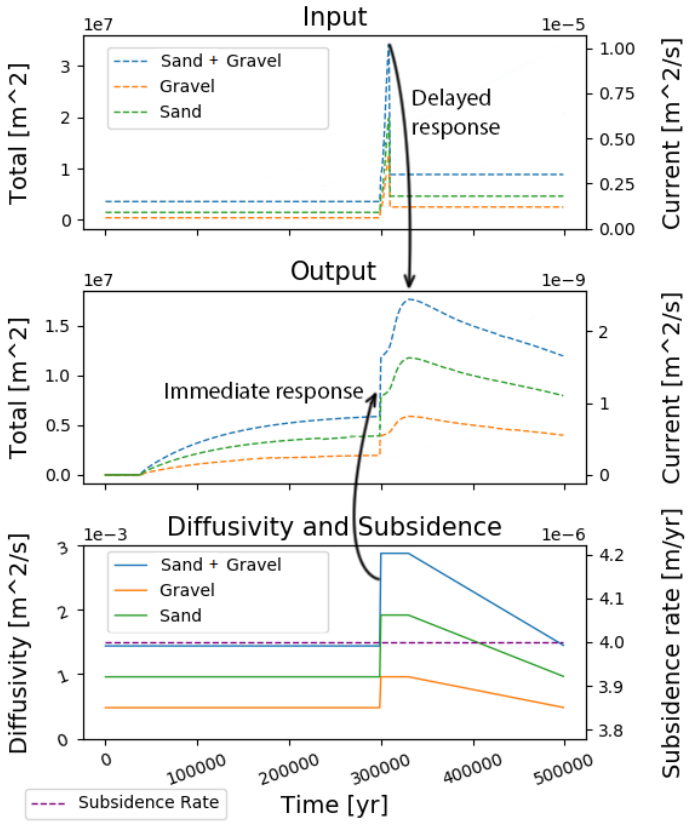

(d) Forcing and transfer system output corresponding to (b). A large initial pulse in input facilitated by stored material in the catchment area. After the stored material is removed from the catchment area, the sediment input falls but remains higher then before.

Figure 12: Two cases producing both a two step transfer system output increase and a gravel front propagation.

5.4 Case study discussion

The results shown in this paper indicate that an increased sediment transportation rate results in an immediate increase in sediment output of the transfer system. This response could explain the sudden increase in detrital sediment input in the marine Zumaia section, congruous with the onset of the PETM. This does not replace the suggestion by Duller et al. (2019) that the increase could be a result of increased advective length, but instead complements it. More sediment may have entered the marine sink which may have travelled further out into the sink basin as a result of the increased advective length, facilitating increased detrital deposition in offshore locations in volume and in lateral extent. Both potential causes however, are a direct result of increased discharge.

The results of this study indicate that the second increase in detrital deposition in marine sections is a response to the increased volume of sediment that is derived from the catchment area. The buffering effect of the transfer system resulted in a delayed output response. This is in agreement with the findings of Castelltort and Van Den Driessche (2003) and Allen (2008).

The delay between the onset of the PETM and the arrival of the conglomerate at intermediate locations in the alluvial system would have been a result of the finite rate of propagation of the gravel front. This delay for any given location in the alluvial system is then determined by (1 the propagation rate of the gravel front and (2 the distance from that location to the gravel front during the onset of the PETM.

The propagation was most likely facilitated by a rapid increase in sediment transport rate. This resulted in a rapid propagation of the gravel front but as soon as the sediment transport rate stopped increasing rapidly and reached stable levels, the propagation stopped. This resulted in a ∼5m thick coarse layer covered by finer sediments.

The sustained high sediment input during the PETM does however result in a large amount of material entering the transfer system. Assuming the PETM did not coincide with a significant increase in subsidence rate, this high input should be recognisable in the transfer system deposits. In the model, this resulted in a second and major increase in the gravel front over the coarse of ∼50myr. This is not recognised in the results of Manners et al. (2013) and Duller et al. (2019). In fact, the Tendrui section in Duller et al. (2019) shows a 30m thick coarse deposit whereas all other deposits showed fine grained deposition during the PETM. In the log of Manners et al. (2013), the Tendrui section also consits of fine grained material. So either the increase in sediment input was was all accommodated in the Tendrui section, a lateral variation the numerical model cannot take into account, or more likely, the bulk of the PETM did not experience a continuously high sediment input. This could conceivably be accomplished through low precipitation following the initial increase, or by increased vegetation facilitated by the change in climate, both of which are not yet properly constrained. A third possibility would be that the PETM was not as persistent on land as it was in the oceans, where the time constraints were obtained.

6 Overall conclusions

Both the general model results and the case study show that alluvial transfer systems and their output are very sensitive to climatic forcing, also those that are very short lived. Variations in sediment input from the catchment area are buffered by the transfer system, resulting in a dampened and phase shifted transfer system output signal. Such changes in sediment input are however generally accompanied by synchronised increases in discharge. This change in discharge directly affects the sediment transport rate within the transfer system. Such increases in sediment transport rate have a very direct effect on the sediment output of the transfer system. The results presented in this paper suggest therefore that, while input signals form the catchment area are indeed buffered by the transfer system, the transfer system output directly reflects both long and rapid changes in climatic forcing, facilitated by changes in discharge.

Variations in climatic forcing can also be recorded within alluvial system deposits through variations in the location of the gravel front and through grain size variations of the deposits. Distinctive propagation of the gravel front can occur in two scenarios: (1 a prolonged scarcity of new sediment input allows coarse material to travel downstream, for it is not being covered by or diluted with newly arriving sediment or (2 a rapidly increasing discharge over input ratio can transport coarse material downstream before it is covered by newly arriving sediment.

References

Allen, P. A. (2008). Time scales of tectonic landscapes and their sediment routing systems. *Geological Society, London, Special Publications*, 296(1):7–28.

Bowen, G. J., Clyde, W. C., Koch, P. L., Ting, S., Alroy, J., Tsubamoto, T., Wang, Y., and Wang, Y. (2002). Mammalian dispersal at the paleocene/eocene boundary. *Science*, 295(5562):2062–2065.

Castelltort, S. and Van Den Driessche, J. (2003). How plausible are high-frequency sediment supply-driven cycles in the stratigraphic record? *Sedimentary geology*, 157(1-2):3–13.

Clechenko, E. R., Kelly, D. C., Harrington, G. J., and Stiles, C. A. (2007). Terrestrial records of a regional weathering profile at the paleocene-eocene boundary in the williston basin of north dakota. *GSA Bulletin*, 119(3-4):428–442.

Culling, W. (1960). Analytical theory of erosion. *The Journal of Geology*, 68(3):336–344.

Domingo, L., López-Martínez, N., Leng, M. J., and Grimes, S. T. (2009). The paleocene–eocene thermal maximum record in the organic matter of the claret and tendruy continental sections (south-central pyrenees, lleida, spain). *Earth and Planetary Science Letters*, 281(3-4):226–237.

Duller, R. A., Armitage, J. J., Manners, H. R., Grimes, S., and Jones, T. D. (2019). Delayed sedimentary response to abrupt climate change at the paleocene-eocene boundary, northern spain. *Geology*, 47(2):159–162.

Flemings, P. B. and Jordan, T. E. (1989). A synthetic stratigraphic model of foreland basin development. *Journal of Geophysical Research: Solid Earth*, 94(B4):3851–3866.

Foreman, B. (2014). Climate-driven generation of a fluvial sheet sand body at the paleocene–eocene boundary in northwest wyoming (usa). *Basin Research*, 26(2):225–241.

Foreman, B. Z., Heller, P. L., and Clementz, M. T. (2012). Fluvial response to abrupt global warming at the palaeocene/eocene boundary. *Nature*, 491(7422):92.

Ganti, V., Lamb, M., and McElroy, B. (2014). Quantitative bounds on morphodynamics and implications for reading the sedimentary record, nat. commun., 5, 1–7.

Jerolmack, D. J. and Paola, C. (2010). Shredding of environmental signals by sediment transport. *Geophysical Research Letters*, 37(19).

John, C. M., Banerjee, N. R., Longstaffe, F. J., Sica, C., Law, K. R., and Zachos, J. C. (2012). Clay assemblage and oxygen isotopic constraints on the weathering response to the paleocene-eocene thermal maximum, east coast of north america. *Geology*, 40(7):591–594.

Kennett, J. P. and Stott, L. (1991). Abrupt deep-sea warming, palaeoceanographic changes and benthic extinctions at the end of the palaeocene. *Nature*, 353(6341):225.

Kenyon, P. and Turcotte, D. (1985). Morphology of a delta prograding by bulk sediment transport. *Geological Society of America Bulletin*, 96(11):1457–1465.

Kraus, M. J., Woody, D. T., Smith, J. J., and Dukic, V. (2015). Alluvial response to the paleocene–eocene thermal maximum climatic event, polecat bench, wyoming (usa). *Palaeogeography, Palaeoclimatology, Palaeoecology*, 435:177–192.

Manners, H. R., Grimes, S. T., Sutton, P. A., Domingo, L., Leng, M. J., Twitchett, R. J., Hart, M. B., Jones, T. D., Pancost, R. D., Duller, R., et al. (2013). Magnitude and profile of organic carbon isotope records from the paleocene–eocene thermal maximum: Evidence from northern spain. *Earth and Planetary Science Letters*, 376:220–230.

Marr, J., Swenson, J., Paola, C., and Voller, V. (2000). A two-diffusion model of fluvial stratigraphy in closed depositional basins. *Basin Research*, 12(3-4):381–398.

Paola, C., Heller, P. L., and Angevine, C. L. (1992). The large-scale dynamics of grain-size variation in alluvial basins, 1: Theory. *Basin Research*, 4(2):73–90.

Paola, C. and Voller, V. R. (2005). A generalized exner equation for sediment mass balance. *Journal of Geophysical Research: Earth Surface*, 110(F4).

Quiquerez, A., Allemand, P., and Dromart, G. (2000). Dibafill: a 3-d two-lithology diffusive model for basin infilling. *Computers & Geosciences*, 26(9-10):1029–1042.

Rivenaes, J. C. (1992). Application of a dual-lithology, depth-dependent diffusion equation in stratigraphic simulation. *Basin Research*, 4(2):133–146.

Rivenaes, J. C. (1997). Impact of sediment transport efficiency on large-scale sequence architecture: results from stratigraphic computer simulation. *Basin Research*, 9(2):91–105.

Röhl, U., Westerhold, T., Bralower, T. J., and Zachos, J. C. (2007). On the duration of the paleocene-eocene thermal maximum (petm). *Geochemistry, Geophysics, Geosystems*, 8(12).

Romans, B. W., Castelltort, S., Covault, J. A., Fildani, A., and Walsh, J. (2016). Environmental signal propagation in sedimentary systems across timescales. *Earth-Science Reviews*, 153:7–29.

Schmitz, B. and Pujalte, V. (2003). Sea-level, humidity, and land-erosion records across the initial eocene thermal maximum from a continental-marine transect in northern spain. *Geology*, 31(8):689–692.

Schmitz, B. and Pujalte, V. (2007). Abrupt increase in seasonal extreme precipitation at the paleocene-eocene boundary. *Geology*, 35(3):215–218.

Simpson, G. and Castelltort, S. (2012). Model shows that rivers transmit high-frequency climate cycles to the sedimentary record. *Geology*, 40(12):1131–1134.

Sinclair, H., Coakley, B., Allen, P., and Watts, A. (1991). Simulation of foreland basin stratigraphy using a diffusion model of mountain belt uplift and erosion: an example from the central alps, switzerland. *Tectonics*, 10(3):599–620.

Slingerland, R. and Kump, L. (2011). *Mathematical Modeling of Earth's Dynamical Systems: A Primer*. Princeton University Press.

Van Den Berg Van Saparoea, A., Postma, G., Hampson, G., Steel, R., Burgess, P., Dalrymple, R., et al. (2008). Control of climate change on the yield of river systems. *Recent advances in models of siliciclastic shallow-marine stratigraphy*.

Watkins, S. E., Whittaker, A. C., Bell, R. E., McNeill, L. C., Gawthorpe, R. L., Brooke, S. A., and Nixon, C. W. (2018). Are landscapes buffered to high-frequency climate change? a comparison of sediment fluxes and depositional volumes in the corinth rift, central greece, over the past 130 ky. *Bulletin*, 131(3-4):372–388.

Westerhold, T., Röhl, U., Wilkens, R., Gingerich, P. D., Clyde, W., Wing, S., Bowen, G., and Kraus, M. (2017). Synchronizing early eocene deep-sea and continental records–new cyclostratigraphic age models from the bighorn basin coring project. *Clim. Past Discuss.*

Whipple, K. X., Parker, G., Paola, C., and Mohrig, D. (1998). Channel dynamics, sediment transport, and the slope of alluvial fans: experimental study. *The Journal of Geology*, 106(6):677–694.

Wing, S. L., Harrington, G. J., Smith, F. A., Bloch, J. I., Boyer, D. M., and Freeman, K. H. (2005). Transient floral change and rapid global warming at the paleocene-eocene boundary. *Science*, 310(5750):993–996.

Zachos, J. C., Röhl, U., Schellenberg, S. A., Sluijs, A., Hodell, D. A., Kelly, D. C., Thomas, E., Nicolo, M., Raffi, I., Lourens, L. J., et al. (2005). Rapid acidification of the ocean during the paleocene-eocene thermal maximum. *Science*, 308(5728):1611–1615.

Zachos, J. C., Wara, M. W., Bohaty, S., Delaney, M. L., Petrizzo, M. R., Brill, A., Bralower, T. J., and Premoli-Silva, I. (2003). A transient rise in tropical sea surface temperature during the paleocene-eocene thermal maximum. *Science*, 302(5650):1551–1554.

Zhang, J., Burgess, P. M., Granjeon, D., and Steel, R. (2019). Can sediment supply variations create sequences? insights from stratigraphic forward modelling. *Basin Research*, 31(2):274–289.

Appendices

A Supporting figures

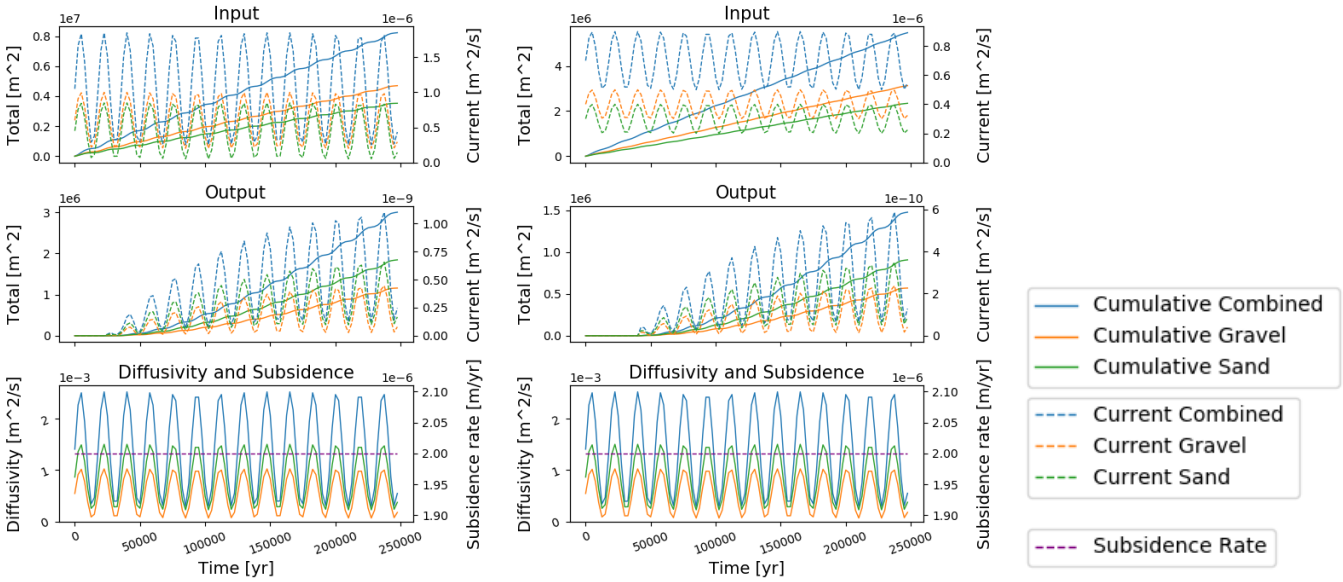

(a) High input amplitude (b) Low input amplitude (c) Legend

Figure 13: Forcing and transfer system output corresponding to figure 8

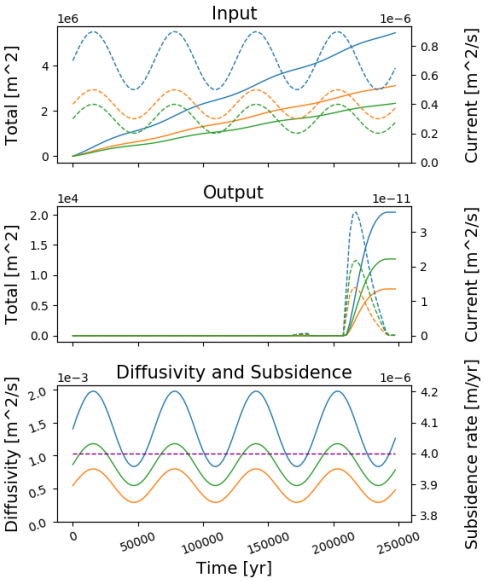

(a) Low input amplitude

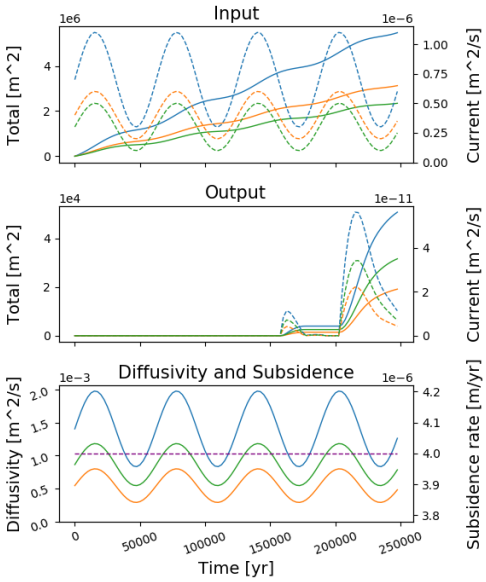

(b) High input amplitude

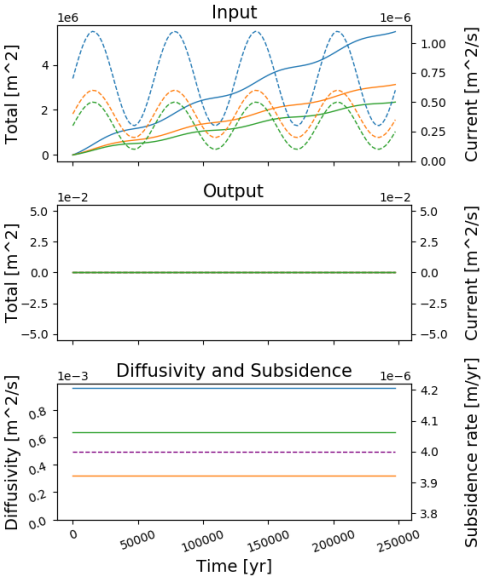

(c) High input amplitude, no diffusion variation

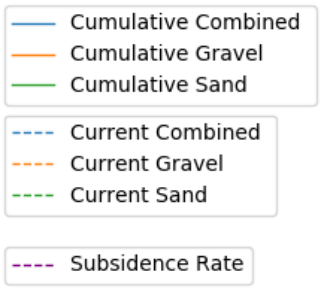

(d) Legend

Figure 14: Forcing and transfer system output corresponding to the scenarios shown in figure 9.

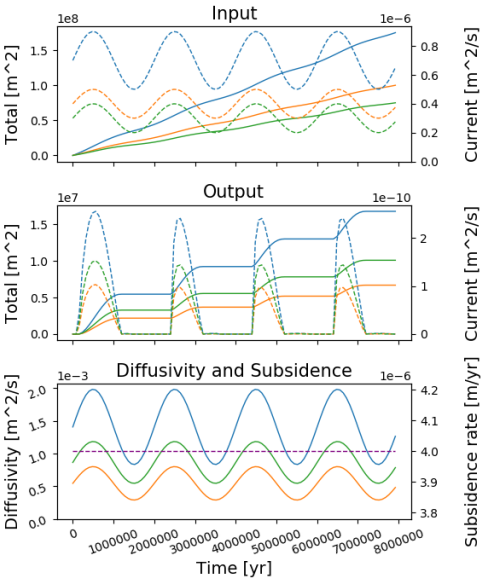

(a) Low input amplitude

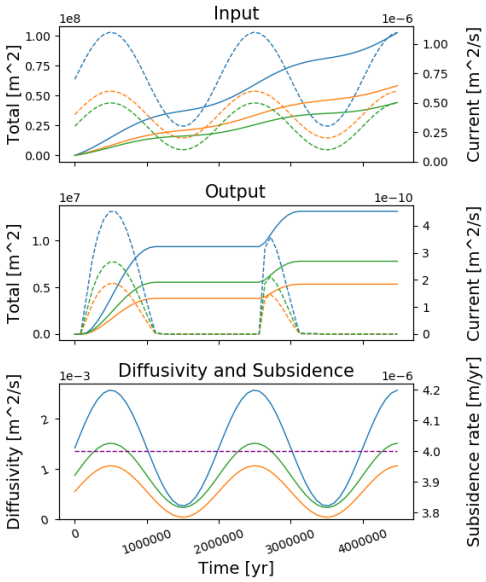

(b) High input amplitude and high diffusion amplitude

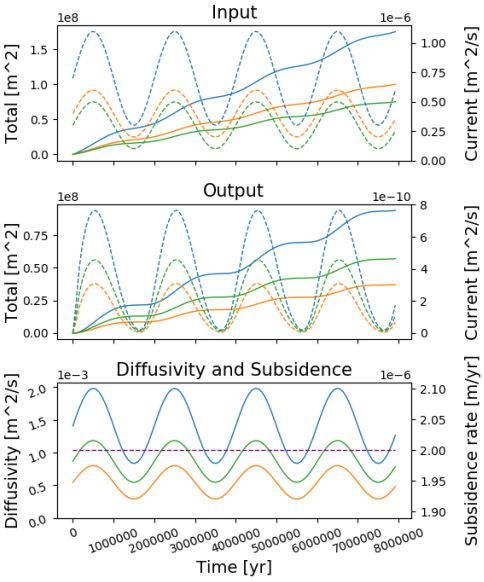

(c) High input amplitude and low subsidence

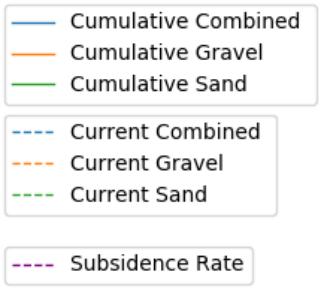

(d) Legend

Figure 15: Forcing and transfer system output corresponding to the scenarios shown in figure 10.

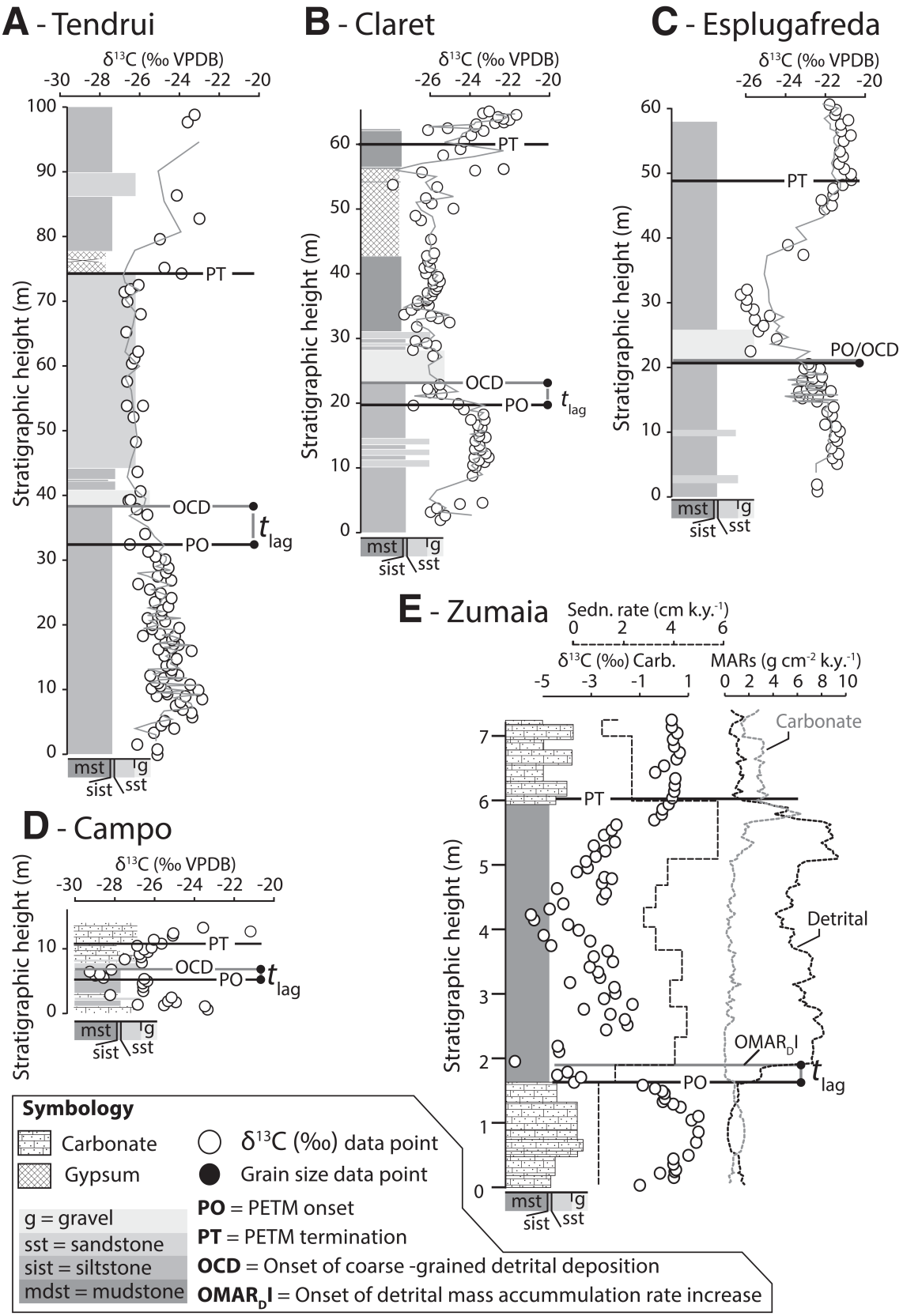

Figure 16: The sedimentary logs corresponding to the locations in figure 11, composed by Duller et al. (2019).

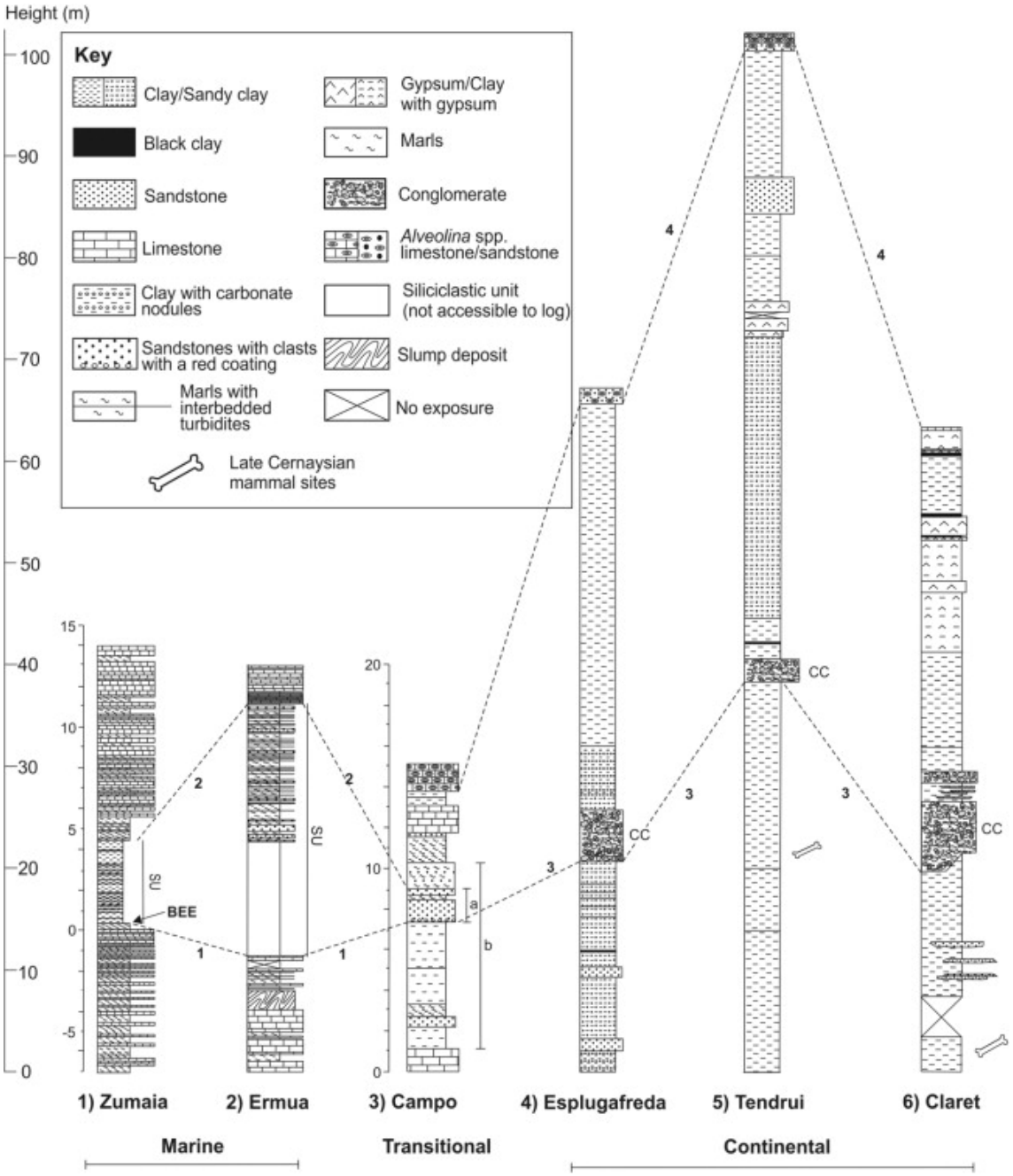

Figure 17: The sedimentary logs corresponding to the locations in figure 11, composed by Manners et al. (2013)